

The calibration of the intramolecular nitrogen isotope distribution in nitrous oxide measured by isotope ratio mass spectrometry[†]

Marian B. Westley^{1*,†}, Brian N. Popp² and Terri M. Rust²

¹Department of Oceanography, University of Hawaii, Honolulu, HI, USA

²Department of Geology and Geophysics, University of Hawaii, Honolulu, HI, USA

Received 9 August 2006; Revised 6 November 2006; Accepted 9 November 2006

Two alternative approaches for the calibration of the intramolecular nitrogen isotope distribution in nitrous oxide using isotope ratio mass spectrometry have yielded a difference in the ¹⁵N site preference (defined as the difference between the $\delta^{15}\text{N}$ of the central and end position nitrogen in NNO) of tropospheric N₂O of almost 30%. One approach is based on adding small amounts of labeled ¹⁵N₂O to the N₂O reference gas and tracking the subsequent changes in *m/z* 30, 31, 44, 45 and 46, and this yields a ¹⁵N site preference of $46.3 \pm 1.4\%$ for tropospheric N₂O. The other involves the synthesis of N₂O by thermal decomposition of isotopically characterized ammonium nitrate and yields a ¹⁵N site preference of $18.7 \pm 2.2\%$ for tropospheric N₂O. Both approaches neglect to fully account for isotope effects associated with the formation of NO⁺ fragment ions from the different isotopic species of N₂O in the ion source of a mass spectrometer. These effects vary with conditions in the ion source and make it impossible to reproduce a calibration based on the addition of isotopically enriched N₂O on mass spectrometers with different ion source configurations. These effects have a much smaller impact on the comparison of a laboratory reference gas with N₂O synthesized from isotopically characterized ammonium nitrate. This second approach was successfully replicated and leads us to advocate the acceptance of the site preference value $18.7 \pm 2.2\%$ for tropospheric N₂O as the provisional community standard until further independent calibrations are developed and validated. We present a technique for evaluating the isotope effects associated with fragment ion formation and revised equations for converting ion signal ratios into isotopomer ratios. Published in 2007 John Wiley & Sons, Ltd.

Nitrous oxide (N₂O) is a potent greenhouse gas in the troposphere¹ and produces NO that interacts destructively with ozone in the stratosphere.² With abundant molecular masses identical to those of carbon dioxide (i.e. 44, 45 and 46), N₂O is easily analyzed by isotope ratio mass spectrometry (IRMS). Measurements of the ¹⁵N and ¹⁸O content of N₂O have been used to evaluate its microbial sources and sinks in soils^{3,4} and the ocean,^{5–7} and to quantify its destruction by photolysis in the stratosphere.⁸ Unlike CO₂, N₂O is an asymmetric molecule with two nonequivalent nitrogen atoms whose isotopic substitution forms distinct isotopomers even when the molecular masses are identical. Yung and Miller⁹ argued that, because of small

differences in their zero point energies, ¹⁴N¹⁵N¹⁶O and ¹⁵N¹⁴N¹⁶O should undergo photolysis in the stratosphere at significantly different rates. The IRMS techniques in use at that time could not distinguish these different forms of mass 45 N₂O, and thus the mechanism of the single most important sink term for atmospheric N₂O remained elusive.

Over 50 years ago, physical chemists studying the production of N₂O from isotopically enriched ammonium nitrate quantified the relative yields of ¹⁴N¹⁵N¹⁶O and ¹⁵N¹⁴N¹⁶O by measuring the ion beam signals at *m/z* (mass-to-charge ratio) 30 and 31 produced by NO⁺ fragments formed during electron ionization in the ion source of an isotope ratio monitoring mass spectrometer.¹⁰ However, it was only recently that two groups established an IRMS technique for determining the relative abundance of these isotopomers in naturally occurring N₂O.^{11,12} The technique is based on monitoring both the molecular N₂O⁺ and the fragment NO⁺ ions using a mass spectrometer that can simultaneously measure *m/z* 44, 45, 46, 30 and 31,¹³ or by performing two sequential measurements on the same

*Correspondence to: M. B. Westley, Geophysical Fluid Dynamics Laboratory, National Oceanic and Atmospheric Administration, 201 Forrestal Road, Princeton, NJ 08540-6649, USA.

E-mail: marian.westley@noaa.gov

[†]Current address: Geophysical Fluid Dynamics Laboratory, National Oceanic and Atmospheric Administration, 201 Forrestal Road, Princeton, NJ 08540-6649, USA.

[‡]This article is a U.S. Government work and is in the public domain in the U.S.A.

Contract/grant sponsor: National Science Foundation; contract/grant number: OCE-0240787.

sample, one monitoring molecular ions and another monitoring fragment ions.¹¹

As predicted,⁹ this new analytical tool has rapidly improved our understanding of the photolysis of N₂O in the stratosphere^{14–17} and the isotopic imprint of the back flux of N₂O from the stratosphere into the troposphere such that 'net stratospheric fluxes should be considered well quantified'.¹⁸ The site-specific ¹⁵N analysis of N₂O has been of great interest to the biogeochemical community since the two major biological sources of N₂O, microbial nitrification and denitrification, often produce N₂O that is impossible to distinguish by conventional IRMS. This is because the isotopic composition of N₂O is influenced by the isotopic composition of its precursors and the isotopic fractionations associated with N₂O formation by nitrification and denitrification are similar.^{19–21} However, Toyoda *et al.*²² argued that the distribution, or site preference (SP $\equiv \delta^{15}\text{N}^{\alpha} - \delta^{15}\text{N}^{\beta}$, where α and β refer to the central and end position nitrogen, respectively), of ¹⁵N within the N₂O molecule should be largely a function of reaction mechanism and independent of source composition. This has been demonstrated in studies with pure strains of nitrifying and denitrifying bacteria.^{23–26} The additional dimension of site preference has greatly enhanced field studies of N₂O cycling in the oceans^{22,27–29} and in soils.^{30,31}

Unfortunately, the adoption of N₂O isotopomer measurements by other laboratories is currently hindered by a large discrepancy in the calibration of position-dependent nitrogen isotope ratios. Precise measurements by IRMS require frequent comparison of the sample with a reference gas of known isotopic composition. There is no internationally accepted N₂O standard gas and, while reference gases can be traced to primary standards by chemical conversion of N₂O into N₂ and CO₂,^{5,32,33} all position-dependent information is lost in this process. Other methods must be applied to calibrate the site preference of the N₂O reference gas used in the IRMS analysis. Two approaches have been advocated: comparison with mixtures of the reference gas with trace additions of isotopically labeled N₂O,^{23,34} and synthesis of N₂O by thermal decomposition of isotopically characterized ammonium nitrate.¹¹ These two approaches have yielded a difference in the ¹⁵N site preference of tropospheric N₂O of almost 30‰: 46.3 ± 1.4‰ by tracer mixing³⁴ vs. 18.7 ± 2.2‰ by synthesis from ammonium nitrate.¹¹ The discrepancy has led other groups either to choose to intercalibrate with one laboratory rather than the other,²⁴ or to compare their data with data from tropospheric N₂O, which can then be referenced to either scale.¹⁸

We set out to replicate both calibration approaches in order to identify the source of the discrepancy in the reported site preference of tropospheric N₂O. First, we calibrated our laboratory reference gas, identified as UH1-N₂O, against N₂ and CO₂ using conventional offline techniques. We then compared our unmixed reference gas with tracer-enhanced mixtures following the method of Kaiser *et al.*³⁴ and using a mass 46 tracer (i.e. ¹⁵N¹⁵N¹⁶O) and two mass 45 tracers (¹⁴N¹⁵N¹⁶O and ¹⁵N¹⁴N¹⁶O). Finally, we compared our reference gas with samples of N₂O synthesized by the thermal decomposition of

ammonium nitrate, following Toyoda and Yoshida¹¹ with minor modifications.

In the course of this work, we identified isotope effects associated with the formation of fragment ions by electron ionization in the ion source of a mass spectrometer. Such effects are to be expected since isotopic substitution leads to differences in zero point energies and thus to differences in the energy necessary to dissociate isotopically substituted molecules into fragments.³⁵ Isotope effects of fragment ion formation were documented by Begun and Landau³⁶ in their study of the isotopic rearrangement of N₂O molecules following electron ionization. Further theoretical work by Lorquet and Cadet³⁷ demonstrated that there are several possible routes to the NO⁺ fragment ion from N₂O⁺ in an excited state, and Märk *et al.*³⁸ documented the production of NO⁺ ions both by unimolecular decay from a metastable intermediate and by collision-induced decomposition. The existence of multiple pathways to the NO⁺ fragment ion indicates that an IRMS measurement based on the ratio of NO⁺ fragments will be sensitive to ion source conditions including vapor pressure (which affects collision frequency), ionizing energy (which affects the distribution of excited energy states) and accelerating voltage (which affects the time spent in the ion source). By examining the relative yields of NO⁺ fragment ions from our laboratory reference gas and ¹⁵N-enriched tracer gases generated under different ion source conditions, we confirm that the different isotopic species of N₂O form fragment ions at slightly different rates, and that these rates are affected by conditions in the ion source. In this paper we show that the current discrepancy in the calibration of position-dependent nitrogen isotope ratios in N₂O stems from a failure to include all the relevant isotope effects associated with fragment ion formation in the calculation of isotopomer abundances from combined measurements of N₂O molecular and fragment ions. This oversight has a large impact on any measurements that include ¹⁵N-enriched mixtures and makes it impossible to replicate the calibration approach described by Kaiser *et al.*³⁴ on a mass spectrometer with a different ion source configuration from that used in the original work. The oversight has a much smaller impact on a calibration based on the synthesis of N₂O from isotopically characterized ammonium nitrate since the same calculations for transforming ion signals into isotopomer ratios are applied equally to the reference and the sample gases.

THEORY

We adopt the convention of Toyoda and Yoshida¹¹ and designate the central nitrogen position as α and the end position as β , such that:

$${}^{15}\text{R}^{\alpha} = [{}^{14}\text{N}{}^{15}\text{N}{}^{16}\text{O}]/[{}^{14}\text{N}{}^{14}\text{N}{}^{16}\text{O}] \quad (1)$$

and

$${}^{15}\text{R}^{\beta} = [{}^{15}\text{N}{}^{14}\text{N}{}^{16}\text{O}]/[{}^{14}\text{N}{}^{14}\text{N}{}^{16}\text{O}] \quad (2)$$

Following Toyoda and Yoshida¹¹ and Kaiser *et al.*,³⁴ the molecular isotopic ratios can be expressed as:

$$^{45}\text{R} = ^{15}\text{R}^\alpha + ^{15}\text{R}^\beta + ^{17}\text{R} \quad (3)$$

$$^{46}\text{R} = (^{15}\text{R}^\alpha + ^{15}\text{R}^\beta)^{17}\text{R} + ^{18}\text{R} + ^{15}\text{R}^\alpha + ^{15}\text{R}^\beta \quad (4)$$

We assume covariance of ¹⁷O and ¹⁸O following Kaiser *et al.*:³³

$$^{17}\text{R} = 0.00937035(^{18}\text{R})^{0.516} \quad (5)$$

Monitoring ion currents at *m/z* 44, 45 and 46 yields the oxygen isotope ratios, ¹⁸R and ¹⁷R, and the average nitrogen isotope ratio, (¹⁵R^α + ¹⁵R^β)/2, defined as the 'bulk' nitrogen isotope ratio,¹¹ or ¹⁵R^{bulk}. (We can solve Eqn. (4) by assuming that ¹⁵R^α = ¹⁵R^β: this approximation in the cross term has a negligible impact on the calculation of the much larger ¹⁸R term; see, e.g., Breninkmeijer *et al.*³⁹) In order to determine ¹⁵R^α and ¹⁵R^β, we monitor the abundance of NO⁺ fragment ions in the ion beams at *m/z* 30 and 31. Unfortunately, the relationship between ³¹R and ¹⁵R^α and ¹⁵R^β is not straightforward. Friedman and Bigeleisen¹⁰ identified a molecular rearrangement process that occurs on electron ionization and yields a significant proportion (around 7%) of fragment ions containing the 'wrong' nitrogen atom, i.e. ¹⁴N¹⁵N¹⁶O yields ¹⁴N¹⁶O⁺ ions and, conversely, ¹⁵N¹⁴N¹⁶O yields ¹⁵N¹⁶O⁺ ions. Thus the *m/z* 31 ion beam will contain, in addition to ¹⁴N¹⁷O⁺, ¹⁵N¹⁶O⁺ from both ¹⁵N-containing isotopomers, and the *m/z* 30 beam will contain ¹⁴N¹⁶O⁺ from both ¹⁵N-containing isotopomers as well as from ¹⁴N¹⁴N¹⁶O.

Toyoda and Yoshida¹¹ define ³¹R as follows:

$$^{31}\text{R} = ^{15}\text{R}^\alpha + ^{17}\text{R} \quad (6)$$

They correct for rearrangement by defining a 'rearrangement fraction', γ , as 'the fraction of NO⁺ bearing β nitrogen of the initial N₂O to the total NO⁺ formed', such that:

$$^{15}\text{R}_{\text{observed}}^\alpha = (1 - \gamma)^{15}\text{R}^\alpha + \gamma^{15}\text{R}^\beta \quad (7)$$

Combining Eqns. (6) and (7) yields:

$$^{31}\text{R} = (1 - \gamma)^{15}\text{R}^\alpha + \gamma^{15}\text{R}^\beta + ^{17}\text{R} \quad (8)$$

In their expression for ³¹R, Kaiser *et al.*³⁴ include the contribution of ¹⁵N¹⁵N¹⁶O, ¹⁴N¹⁵N¹⁷O and ¹⁵N¹⁴N¹⁷O to *m/z* 31, and the contributions of ¹⁵N¹⁴N¹⁶O and ¹⁴N¹⁵N¹⁶O to *m/z* 30:

$$^{31}\text{R} = \frac{(1 - \gamma)^{15}\text{R}^\alpha + \gamma^{15}\text{R}^\beta + ^{15}\text{R}^\alpha \cdot ^{15}\text{R}^\beta + ^{17}\text{R}(1 + \gamma^{15}\text{R}^\alpha + (1 - \gamma)^{15}\text{R}^\beta)}{1 + \gamma^{15}\text{R}^\alpha + (1 - \gamma)^{15}\text{R}^\beta} \quad (9)$$

We note that Eqns. (8) and (9) both contain the following implicit assumptions: (1) the different isotopic species of N₂O form fragment ions at equal rates; and (2) the fraction of ions formed by rearrangement is identical for ¹⁵N¹⁴NO and ¹⁴N¹⁵NO. Rejecting these assumptions, we find:

$$^{31}\text{R} = \frac{a_{31}^{15}\text{R}^\alpha + b_{31}^{15}\text{R}^\beta + c_{31}^{15}\text{R}^\alpha \cdot ^{15}\text{R}^\beta + ^{17}\text{R}(d_{31} + e_{31}^{15}\text{R}^\alpha + f_{31}^{15}\text{R}^\beta)}{1 + a_{30}^{15}\text{R}^\alpha + b_{30}^{15}\text{R}^\beta + c_{30}^{15}\text{R}^\alpha \cdot ^{15}\text{R}^\beta} \quad (10)$$

The constants a_{31} and a_{30} represent the relative yields of *m/z* 31 and *m/z* 30 fragments, respectively, from ¹⁴N¹⁵N¹⁶O; b_{31} and b_{30} represent the relative yields of *m/z* 31 and *m/z* 30 fragments from ¹⁵N¹⁴N¹⁶O; c_{31} and c_{30} represent the relative yields of *m/z* 31 and *m/z* 30 fragments from ¹⁵N¹⁵N¹⁶O (the *m/z* 30 fragments are ¹⁵N₂⁺ ions); and d_{31} , e_{31} and f_{31} represent the relative yields of *m/z* 31 fragments from ¹⁴N¹⁴N¹⁷O, ¹⁴N¹⁵N¹⁷O and ¹⁵N¹⁴N¹⁷O. In each case, these constants are normalized to the relative yield of *m/z* 30 fragments from ¹⁴N¹⁴N¹⁶O.

Comparing Eqn. (10) with Eqns. (8) and (9), we see that Toyoda and Yoshida¹¹ and Kaiser *et al.*³⁴ assume that b_{31} and a_{30} are identical; i.e. the relative yield of *m/z* 31 fragment ions from ¹⁵N¹⁴N¹⁶O is identical to the relative yield of *m/z* 30 fragment ions from ¹⁴N¹⁵N¹⁶O, and can be expressed as a single 'rearrangement factor' or 'scrambling coefficient'. In addition, both groups assume that b_{30} and a_{31} are identical and equal to $1 - b_{31}$ or $1 - a_{30}$. The implication of these assumptions is that ¹⁴N¹⁵N¹⁶O and ¹⁵N¹⁴N¹⁶O have an equal likelihood of forming NO⁺ ions (both normal and rearranged) as ¹⁴N¹⁴N¹⁶O and as each other. Likewise, both groups assume that ¹⁴N¹⁴N¹⁷O forms *m/z* 31 ions at the same rate as ¹⁴N¹⁴N¹⁶O forms *m/z* 30 ions, and Kaiser *et al.*³⁴ make the further assumption that ¹⁴N¹⁵N¹⁷O and ¹⁵N¹⁴N¹⁷O form fragment ions at the same rate as ¹⁴N¹⁵N¹⁶O and ¹⁵N¹⁴N¹⁶O (Toyoda and Yoshida¹¹ ignore ¹⁴N¹⁵N¹⁷O and ¹⁵N¹⁴N¹⁷O, which should be very rare in naturally occurring N₂O). While Toyoda and Yoshida¹¹ ignore ¹⁵N¹⁵N¹⁶O (the abundance of this isotopologue should also be very low in naturally occurring N₂O), Kaiser *et al.*³⁴ include it but assume that c_{31} is equal to 1; i.e. the relative yield of *m/z* 31 fragment ions from ¹⁵N¹⁵N¹⁶O is identical to the relative yield of *m/z* 30 fragment ions from ¹⁴N¹⁴N¹⁶O. There is no *a priori* reason to assume that the different isotopic species of N₂O will display uniform fragmentation behavior, and thus we reject these assumptions. In the following sections we demonstrate that there are isotope effects associated with the fragmentation of N₂O molecules in the ion source of a mass spectrometer, that different isotopic species form fragment ions at different rates, and that these differences are affected by conditions in the ion source, including ionization energy, accelerating voltage and source pressure. We then evaluate the impacts of these

isotope effects on the two different calibration approaches, tracer mixing and comparison with N₂O synthesized from ammonium nitrate. In particular, we will demonstrate that the tracer addition calibration approach presented by Kaiser *et al.*³⁴ depends critically on the assumption that c_{31}

is equal to 1, an assumption that is not borne out by our measurements.

EXPERIMENTAL

Mass spectra of reference and tracer gases

To demonstrate that there are isotope effects associated with the formation of fragment ions, we measured fragment ion production by four gases: our laboratory reference gas, UH1-N₂O (Grade 4.5 N₂O, BOC Gases, Murray Hill, NJ, USA) and three ¹⁵N-labeled gases purchased from ICON Isotopes (Summit, NJ, USA), herein referred to as ICON-¹⁴N¹⁵N¹⁶O, ICON-¹⁵N¹⁴N¹⁶O and ICON-¹⁵N¹⁵N¹⁶O. We measured these gases on two different mass spectrometers, a ThermoFinnigan Delta Plus XP and a Finnigan MAT 252 (both from Thermo Electron, Waltham, MA, USA). In each case, we compared peaks from a tracer gas loaded into one bellows with those from UH1-N₂O loaded into the other bellows, keeping all conditions, including ion source pressure, as closely matched as possible. All peaks were measured on a single Faraday cup by peak jumping between relevant *m/z* values and centering each peak. Measurements were performed five times each, alternating between the tracer gas and UH1-N₂O with each measurement cycle. The measurements from the MAT 252 were obtained under normal operating conditions, using an ionization energy of 60 eV and an ion accelerating voltage of 9.8 kV. Taking advantage of two Faraday cups with peak centering capability but different sensitivities on the MAT 252, we compared the relative yields of *m/z* 30 and *m/z* 31 ions from our tracer gases and UH1-N₂O at two ion source pressure values: 7×10^{-9} and 1.5×10^{-7} mbar. Using the Delta Plus XP, we examined the effect of changing ionization energy and accelerating voltage. In the case of changing the accelerating voltage, we measured the maximum intensity of each peak using a magnetic field scan, holding the accelerating voltage constant. (Normal peak centering on the Delta Plus XP is performed by holding the magnetic step value constant and changing the accelerating voltage.) All tests on each gas pair were performed in a single day.

Calibration of $\delta^{15}\text{N}^{\text{bulk}}$ and $\delta^{18}\text{O}$ in the laboratory reference gas

We evaluated the ¹⁸O and average ¹⁵N content of UH1-N₂O using typical offline techniques. We used the approach of Ueda *et al.*³² to convert our reference gas into N₂ (reduction with copper wire heated to 400°C for 4 h) and the approach of Kim and Craig,⁵ as modified by Kaiser *et al.*,³³ to convert our reference gas into CO₂ and N₂ (graphite wrapped in platinum wire mesh heated to 690–713°C for 1 h). We then measured the resulting gases against laboratory reference gases of N₂ and CO₂ traced to standard material provided by the National Institute of Standards and Technology, USA. We found inconsistent results for $\delta^{18}\text{O}$ -CO₂ so repeated the exercise with a slight modification: after 1 h of heating, we separated the CO₂ and potentially residual N₂O from N₂ and potentially residual CO, removed the latter gases, and returned the CO₂ fraction to the hot chamber for a further 10 min. We measured five aliquots of N₂ generated using the Ueda *et al.*³² technique, eight of N₂

following Kaiser *et al.*,³³ and five of CO₂ following Kaiser *et al.*³³ with 10 min of additional heating. We also transferred aliquots of UH1-N₂O into 6 mm Pyrex tubes and sent them to the laboratories of Naohiro Yoshida at the Tokyo Institute of Technology, in Yokohama, Japan, and Thomas Röckmann, then at the Max Planck Institute for Nuclear Physics, in Heidelberg, Germany, for comparison with their laboratory reference gases.

Position-dependent ¹⁵N calibration by tracer addition

Kaiser *et al.*³⁴ present a simple calibration technique that uses mixtures of the laboratory reference gas with trace additions of ¹⁵N¹⁵N¹⁶O and tracks the increase in ⁴⁶R and ³¹R relative to unmixed reference gas. In their appendices, they describe similar approaches using trace additions of ¹⁴N¹⁵N¹⁶O and ¹⁵N¹⁴N¹⁶O and tracking increases in ⁴⁵R and ³¹R. We implemented this approach on our ThermoFinnigan Delta Plus XP, an isotope ratio monitoring mass spectrometer with Faraday cups configured to simultaneously measure *m/z* 30, 31, 44, 45 and 46. We used an accelerating voltage of 2.981 kV and an ionization energy of 117.69 eV. UH1-N₂O was the reference gas and the base of the tracer-enhanced mixtures. The tracers added were ICON-¹⁴N¹⁵N¹⁶O, ICON-¹⁵N¹⁴N¹⁶O and ICON-¹⁵N¹⁵N¹⁶O. We created our mixtures by loading our reference gas into both bellows of our dual-inlet system, closing the bellows, evacuating the space around the bellows, then introducing a small amount of tracer gas into this space by injection from a gastight syringe through a rubber septum. We allowed the reference gas in one of the bellows to equilibrate with the tracer gas while keeping the other bellows closed. We then closed both bellows and evacuated the space around them to remove all traces of isotopically enriched gas. We expanded and contracted the bellows containing the mixed gases several times to enhance mixing, and then allowed the gas to equilibrate for a further 5 min before opening both bellows to the switchover valve in preparation for an eight-cycle dual-inlet mode measurement controlled by Isodat-NT software (v.2.0) provided by Thermo Electron. Mixing curves were generated by sequential dilution of the tracer-enhanced gas with additional unmixed reference gas. Creating our gas mixtures directly in the bellows of the mass spectrometer provides the advantage of minimizing the opportunity for introducing impurities (particularly CO₂) during gas transfer. Since the mass spectrometer itself is used to quantify the ratio of tracer gas to reference gas, and since molecular and fragment ions are measured simultaneously, the actual mixing ratios need not be known prior to the measurement.

Calibration by synthesis of N₂O from ammonium nitrate

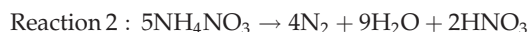
Toyoda and Yoshida¹¹ used the synthesis of N₂O from isotopically characterized ammonium nitrate (NH₄NO₃) to generate a suite of gases against which to calibrate their reference gas. The advantage of this approach is that information on the relative abundance of isotopomers in each synthesized gas sample is obtained independently from the isotopomer measurement itself. Disadvantages of this

approach identified by Kaiser *et al.*³⁴ are the laborious wet chemistry involved in characterizing the starting material and the potential isotope effects associated with the thermal decomposition of NH₄NO₃ to N₂O. We replicated the calibration approach of Toyoda and Yoshida¹¹ in order to assess its usefulness.

According to Friedman and Bigeleisen,¹⁰ the thermal decomposition of NH₄NO₃ to N₂O occurs between 180°C and 300°C and proceeds by a dehydration reaction that preserves the relative positions of the two nitrogen atoms:



Shah and Oza⁴⁰ note the existence of a side reaction that produces N₂:



Brower *et al.*⁴¹ observed variable induction times and capricious reaction rates for the thermal decomposition reaction in the temperature region around 200°C. We experimented with this reaction in evacuated 9 mm Vycor tubes, with and without the addition of water vapor (Friedman and Bigeleisen¹⁰ asserted that water vapor was necessary to induce the reaction although Rosser *et al.*⁴² found it to be an inhibitor), in the temperature range used by Toyoda and Yoshida,¹¹ 225–230°C, and found that even after 5 days of heating, some unreacted NH₄NO₃ often remained. Reports vary as to which temperature leads to an explosive reaction, but since Brower *et al.*⁴¹ observed the reaction in sealed capillary tubes between 200 and 400°C, we chose 360°C as a good compromise between the desire for a fast reaction rate and the imperative of safety.

Five batches of isotopically distinct NH₄NO₃ were prepared by recrystallizing 40 g NH₄NO₃ (Sigma-Ultra, >99.5% purity, Sigma-Aldrich, St. Louis, MO, USA) with and without the addition of tracer ¹⁵N in the form of ammonium chloride (Isotec, >98% ¹⁵N, Sigma-Aldrich) or sodium nitrate (Isotec, >98% ¹⁵N, Sigma-Aldrich). Samples were homogenized and purified by recrystallization: enough distilled, deionized water (DI H₂O) was added to cover the crystals in 50 mL glass centrifuge tubes, which were immersed in a boiling water bath until dissolution occurred, and then immersed in an ice bath until crystals formed and the overlying water could be decanted. The recrystallization was performed four times, twice with the addition of 2 mL aliquots of concentrated, trace-metal-clean nitric acid (to remove halogen impurities known to enhance the relative production of N₂ gas: see Saunders⁴³), followed by two recrystallizations without acid. The resulting crystals were then transferred to clean beakers and dried at 120°C. We isolated the ammonium ion from NH₄NO₃ for isotopic analysis by reaction with aqueous sodium tetraphenylborate (Sigma-Aldrich, >99.5%): 0.5 g sodium tetraphenylborate was dissolved in 20 mL DI H₂O, then 0.1 g of NH₄NO₃ was added, instantaneously forming an insoluble white precipitate of ammonium tetraphenylborate. This precipitate was purified by resuspension in DI H₂O, followed by centrifuging and decanting the supernatant water containing dissolved sodium and nitrate ions. Resuspension and centrifugation were performed three times for each sample of ammonium tetraphenylborate. The resultant precipitate

was dried for several days at 60°C. The prepared and purified NH₄NO₃ and ammonium tetraphenylborate were analyzed isotopically using an online carbon-nitrogen analyzer coupled with an isotope ratio mass spectrometer (Finnigan ConFlo II/Delta Plus, Thermo Electron). Analytical uncertainties in δ¹⁵N values were evaluated by calculating the standard deviations (SDs) from the mean of five analyses of purified NH₄NO₃ and ammonium tetraphenylborate and were found to be ±0.32‰ and ±0.17‰, respectively.

Once dried, 10 mg samples of ammonium nitrate were weighed into precombusted 9 mm Vycor tubes and sealed following evacuation on a vacuum line. The tubes were placed in a preheated combustion furnace at 360°C and allowed to react for 1 h. Tubes were then removed from the oven and cooled to room temperature. The resulting gases, mostly N₂O and N₂, were separated by cryogenic gas distillation on a vacuum line. N₂O was trapped in liquid nitrogen, quantified using a calibrated electronic manometer, and transferred to 6 mm Pyrex sample tubes and flame-sealed. Nitrogen gas was cryogenically trapped with liquid nitrogen on silica gel, quantified with the manometer, and then exposed to copper wire heated to 500°C to remove oxygen. After 20 min, the remaining gas was trapped and quantified a second time, then transferred to 6 mm Pyrex sample tubes using silica gel, and sealed. The samples of N₂ were isotopically characterized using a Finnigan MAT 252 mass spectrometer in dual-inlet mode. The analytical uncertainty (SD of multiple analyses of the same starting material) in δ¹⁵N of N₂ was ±0.54‰. The N₂O samples were measured against our UH1-N₂O reference gas calibrated against N₂ and CO₂ as described above, using the Thermo-Finnigan Delta Plus XP in dual-inlet mode. Between two and six runs were completed for each batch of ammonium nitrate; the highest SD in the resulting δ¹⁵N₂O^{bulk} measurements was ±0.47‰ for three analyses of ammonium nitrate enhanced with ¹⁵NO₃⁺. We assign this value as the analytical uncertainty of this method.

RESULTS AND DISCUSSION

Mass spectra: isotope effects of fragment ion formation

Table 1 summarizes one set of mass spectra obtained for each gas, our UH1-N₂O reference gas and three ¹⁵N-labeled gases, ICON-¹⁴N¹⁵N¹⁶O, ICON-¹⁵N¹⁴N¹⁶O and ICON-¹⁵N¹⁵N¹⁶O, using the ThermoFinnigan Delta Plus XP (2.981 kV accelerating voltage, 117.69 eV ionization energy) to evaluate the presence of impurities. All peaks are normalized such that the sum of the molecular ion signals (i.e. *m/z* 44, 45, 46, 47 and 48) adds up to 100. The absence of peaks at *m/z* 12 shows that there are no C⁺ ions and thus no CO₂ in any of our gases. In addition, we see no *m/z* 49 ions in the mass spectrum of ICON-¹⁵N¹⁵N¹⁶O, which indicates that there is no NO₂⁺ formation (i.e. ¹⁵N¹⁶O¹⁸O⁺), which has been shown by others to interfere with N₂O isotope measurements. From Table 1 we see that UH1-N₂O is 99% mass 44 (¹⁴N¹⁴N¹⁶O), 0.77% mass 45 (¹⁴N¹⁵N¹⁶O, ¹⁵N¹⁴N¹⁶O, ¹⁴N¹⁴N¹⁷O) and 0.22% mass 46 (mostly ¹⁴N¹⁴N¹⁸O). ICON-¹⁴N¹⁵N¹⁶O is 98.2% mass 45, ICON-¹⁵N¹⁴N¹⁶O is 98.7% mass 45, and ICON-¹⁵N¹⁵N¹⁶O is 98.8% mass 46.

Table 1. Mass spectra of each reference gas using a ThermoFinnigan Delta Plus XP mass spectrometer operating at an accelerating voltage of 2.98 kV and an ionization energy of 117.6 eV. All peaks are normalized such that the sum of the molecular ion signals (i.e. m/z 44, 45, 46, 47 and 48) add up to 100

Mass-to-charge ratio	UHI-N ₂ O	ICON- ¹⁴ N ¹⁵ N ¹⁶ O	ICON- ¹⁵ N ¹⁴ N ¹⁶ O	ICON- ¹⁵ N ¹⁵ N ¹⁶ O
Monatomic fragments				
12	0.00	0.00	0.00	0.00
13	0.00	0.00	0.00	0.00
14	5.38	2.45	2.82	0.05
15	0.04	3.01	2.53	5.49
16	2.35	2.34	2.33	2.37
17	0.11	0.10	0.11	0.12
18	0.37	0.34	0.36	0.35
Diatomic fragments				
28	8.70	0.34	0.23	0.27
29	0.08	8.72	9.11	0.18
30	23.98	2.30	21.39	8.94
31	0.11	21.30	2.20	22.84
32	0.36	0.29	0.27	0.31
33	0.00	0.16	0.01	0.05
Molecules				
44	99.01	0.63	0.62	0.04
45	0.77	98.23	98.65	0.92
46	0.22	0.44	0.51	98.78
47	0.00	0.70	0.21	0.04
48	0.00	0.00	0.00	0.21

Table 2 shows fragmentation factors, or the relative yields of m/z 30 and m/z 31 fragments from ICON-¹⁴N¹⁵N¹⁶O, ICON-¹⁵N¹⁴N¹⁶O and ICON-¹⁵N¹⁵N¹⁶O compared with the yield of m/z 30 fragments from UHI-N₂O, under a range of instrument conditions. Values are reported as means and SDs of five cycles of dual-inlet measurements, with switchover valves controlled manually and peak centering performed on each ion beam of interest. Resulting values are normalized to the dominant molecular ion species, which is assigned a value of 100. For each measurement, we correct for impurities following Kaiser *et al.*,³⁴ who purchased similar gases from the same supplier: for ICON-¹⁴N¹⁵N¹⁶O and ICON-¹⁵N¹⁴N¹⁶O, we assume a 0.1% contribution of the unwanted mass 45 isotopomer, and for ICON-¹⁵N¹⁵N¹⁶O, we assume that any non-¹⁷O-derived m/z 45 consists of equal amounts of ¹⁴N¹⁵N¹⁶O and ¹⁵N¹⁴N¹⁶O. We measure the ¹⁸O content of these gases and, following Kaiser *et al.*,³⁴ with confirmation from the manufacturer, assume a normal distribution of ¹⁷O. For UHI-N₂O, we use our knowledge of the ¹⁸O and ¹⁵N content from offline conversion into N₂ and CO₂ following the methods of Kim and Craig⁵ and Ueda *et al.*,³² and assume a normal oxygen distribution and roughly equal amounts of ¹⁴N¹⁵N¹⁶O and ¹⁵N¹⁴N¹⁶O contributing to the m/z 45 ion beam. To correct for the contribution of impurities to fragment ion signals, we use the estimated fragmentation rates from each of our four gases and perform an iterative series of corrections for the contributions of impurities to the fragment ion signals, revising the fragmentation rates after each cycle of corrections. These corrections have a small impact (between 0.5% and 1.5%) on all values except for the relative yield of m/z 30 from ¹⁴N¹⁵N¹⁶O, which in each case is revised downwards by between 8.5% and 9% when we remove the contributions of m/z 30 fragments from ¹⁴N¹⁴N¹⁶O, ¹⁵N¹⁴N¹⁶O and ¹⁵N¹⁵N¹⁶O.

The same series of calculations yields our estimates for the fragmentation factors a_{30} , b_{30} and c_{30} , the relative yields of

m/z 30 ions from ¹⁴N¹⁵N¹⁶O, ¹⁵N¹⁴N¹⁶O and ¹⁵N¹⁵N¹⁶O, respectively, and likewise for a_{31} , b_{31} and c_{31} , the relative yields of m/z 31 ions from ¹⁴N¹⁵N¹⁶O, ¹⁵N¹⁴N¹⁶O and ¹⁵N¹⁵N¹⁶O, respectively. These values are shown in Table 3. For comparison, we show the values for the rearrangement factors, or scrambling coefficients, calculated for ¹⁴N¹⁵N¹⁶O and ¹⁵N¹⁴N¹⁶O in the manner described by Kaiser,⁴⁴ Section 2.4.1: γ^α is the ratio of m/z 30 fragment ions to total NO⁺ fragment ions produced from ¹⁴N¹⁵N¹⁶O and γ^β is the ratio of m/z 31 fragment ions to total NO⁺ fragment ions produced from ¹⁵N¹⁴N¹⁶O. Missing from Table 3 are estimates of d_{31} , e_{31} or f_{31} , the relative yields of m/z 31 ions from ¹⁴N¹⁴N¹⁷O, ¹⁴N¹⁵N¹⁷O and ¹⁵N¹⁴N¹⁷O, respectively, which we cannot obtain without a pure sample of ¹⁷O-enriched N₂O. Instead we assume that ¹⁴N¹⁴N¹⁷O has the same fragmentation rate as ¹⁴N¹⁴N¹⁶O and we ignore the rare isotopologues, ¹⁴N¹⁵N¹⁷O and ¹⁵N¹⁴N¹⁷O. This means that e_{31} and f_{31} are both set to 0 and d_{31} is set to 1. This is probably a safe assumption for natural abundance measurements of the N₂O isotopic species since ¹⁷R is about an order of magnitude smaller than ¹⁵R ^{α} , ¹⁵R ^{β} and ¹⁸R, but we encourage those laboratories with a specific interest in ¹⁷O to evaluate the constants d_{31} , e_{31} or f_{31} explicitly.

From Table 2 it is clear that the yield of NO⁺ fragment ions relative to N₂O⁺ molecular ions is highly variable. For example, the relative yield of NO⁺ fragment ions from ¹⁴N¹⁴N¹⁶O ranges from 19.357 ± 0.009 on the Delta Plus XP (at 2.98 kV and 118 eV) to 35.025 ± 0.028 on the MAT 252 (at 9.8 kV, 60 eV and an in-source pressure of 7×10^{-9} mbar). Decreasing the ionization energy and decreasing the accelerating voltage both cause increases in the relative fragment ion yield for all isotopic species measured on the Delta Plus XP. However, these increases are accompanied by large decreases in total ion yield: in the ionization energy experiment, maximum voltages (i.e. the ion signal from the

Table 2. Relative rate of fragment ion formation from $^{14}\text{N}^{15}\text{N}^{16}\text{O}$, $^{15}\text{N}^{14}\text{N}^{16}\text{O}$ and $^{15}\text{N}^{15}\text{N}^{16}\text{O}$ compared to $^{14}\text{N}^{14}\text{N}^{16}\text{O}$ under a range of instrument conditions. Values are corrected for the contribution of impurities as described in the text and normalized to the dominant molecular ion peak, which is assigned a value of 100. All m/z 30 and 31 ions represent the formation of NO^+ ions except for m/z 30 from $^{15}\text{N}^{15}\text{N}^{16}\text{O}$, which is N_2^+ . Reported values are the means and, in parentheses, standard deviations of five pairs of measurements

Experiment	Test conditions	$^{14}\text{N}^{14}\text{N}^{16}\text{O}$		$^{14}\text{N}^{15}\text{N}^{16}\text{O}$		$^{14}\text{N}^{14}\text{N}^{16}\text{O}$		$^{15}\text{N}^{14}\text{N}^{16}\text{O}$		$^{15}\text{N}^{15}\text{N}^{16}\text{O}$	
		m/z 30	m/z 31	m/z 30	m/z 31	m/z 30	m/z 31	m/z 30	m/z 31	m/z 30	m/z 31
Delta Plus XP with varying ionization energy	2.98 kV, 118 eV 2.98 kV, 90 eV 2.98 kV, 60 eV	20.487 (0.026) 21.086 (0.004) 22.732 (0.072)	18.526 (0.006) 19.052 (0.026) 20.533 (0.047)	1.794 (0.006) 1.827 (0.003) 1.941 (0.005)	19.357 (0.009) 19.763 (0.029) 21.832 (0.038)	17.362 (0.028) 17.717 (0.048) 19.695 (0.164)	1.832 (0.003) 1.866 (0.006) 2.010 (0.018)	20.951 (0.025) 21.543 (0.009) 22.782 (0.042)	7.798 (0.013) 8.079 (0.007) 8.724 (0.132)	19.939 (0.033) 20.533 (0.020) 21.775 (0.018)	
Delta Plus XP with varying accelerating voltage	3.08 kV 2.17 kV	21.627 (0.064) 22.111 (0.029)	19.634 (0.068) 19.859 (0.027)	1.834 (0.012) 1.837 (0.003)	21.392 (0.104) 21.916 (0.076)	19.449 (0.020) 19.962 (0.032)	1.964 (0.004) 2.001 (0.006)	21.707 (0.055) 22.081 (0.050)	8.117 (0.036) 8.285 (0.080)	20.887 (0.056) 21.043 (0.073)	
MAT 252 with varying pressure	1.26 kV 9.8 kV, $60\text{ eV } 7 \times 10^{-9}$ mbar 9.8 kV, $60\text{ eV } 1.5 \times 10^{-7}$ mbar	23.011 (0.106) 34.814 (0.030) 26.959 (0.017)	20.670 (0.065) 31.441 (0.021) 24.337 (0.015)	1.860 (0.003) 3.204 (0.046) 2.186 (0.019)	22.276 (0.155) 35.025 (0.028) 26.929 (0.024)	20.271 (0.028) 32.032 (0.012) 24.152 (0.046)	2.018 (0.003) 3.218 (0.028) 2.388 (0.018)	23.752 (0.165) 35.025 (0.028) 26.686 (0.023)	8.554 (0.015) 14.153 (0.044) 9.639 (0.015)	22.655 (0.082) 32.799 (0.030) 25.563 (0.038)	

Table 3. Fragmentation factors calculated from the pairs of measurements summarized in Table 2. The constants a_{31} and a_{30} represent the relative yield of m/z 31 and m/z 30 fragments, respectively, from $^{14}\text{N}^{15}\text{N}^{16}\text{O}$; b_{31} and b_{30} represent the relative yield of m/z 31 and m/z 30 fragments, respectively, from $^{15}\text{N}^{14}\text{N}^{16}\text{O}$; and c_{31} and c_{30} represent the relative yield of m/z 31 and m/z 30 fragments, respectively, from $^{15}\text{N}^{15}\text{N}^{16}\text{O}$. All values are corrected for the contribution of impurities as described in the text, and all constants are normalized to the relative yield of m/z 30 fragments from $^{14}\text{N}^{14}\text{N}^{16}\text{O}$ measured under the same conditions. All m/z 30 and 31 ions represent the formation of NO^+ ions except for m/z 30 from $^{15}\text{N}^{15}\text{N}^{16}\text{O}$, which is N_2^+ . Reported values are the means and, in parentheses, standard deviations calculated by propagation of errors from five pairs of measurements. For comparison, we show the values for the rearrangement factors, or scrambling coefficients, calculated according to Kaiser.⁴⁴ γ^β is the ratio of m/z 30 fragment ions to total fragment ions produced from $^{14}\text{N}^{15}\text{N}^{16}\text{O}$ and γ^β is the ratio of m/z 31 fragment ions to total fragment ions produced from $^{15}\text{N}^{14}\text{N}^{16}\text{O}$

Instrument model	Test conditions	$^{14}\text{N}^{15}\text{N}^{16}\text{O}$		$^{15}\text{N}^{14}\text{N}^{16}\text{O}$		$^{15}\text{N}^{15}\text{N}^{16}\text{O}$	
		a_{31}	a_{30}	b_{31}	b_{30}	γ^β	c_{31}
Delta Plus XP with varying ionization energy	2.98 kV, 118 eV 2.98 kV, 90 eV 2.98 kV, 60 eV	0.904 (0.001) 0.904 (0.001) 0.903 (0.004)	0.088 (0.000) 0.087 (0.000) 0.085 (0.000)	0.095 (0.000) 0.094 (0.000) 0.092 (0.001)	0.897 (0.002) 0.896 (0.003) 0.902 (0.008)	0.088 (0.000) 0.087 (0.000) 0.086 (0.000)	0.952 (0.002) 0.953 (0.001) 0.956 (0.002)
Delta Plus XP with varying accelerating voltage	XP at 3.08 kV XP at 2.17 kV XP at 1.26 kV	0.903 (0.001) 0.903 (0.001) 0.908 (0.004)	0.092 (0.001) 0.082 (0.001) 0.085 (0.001)	0.092 (0.001) 0.089 (0.001) 0.092 (0.000)	0.915 (0.001) 0.897 (0.002) 0.909 (0.005)	0.091 (0.001) 0.090 (0.001) 0.092 (0.000)	0.936 (0.001) 0.958 (0.002) 0.962 (0.004)
MAT 252 with varying pressure	9.8 kV, $60\text{ eV } 7 \times 10^{-9}$ mbar 9.8 kV, $60\text{ eV } 1.5 \times 10^{-7}$ mbar	0.898 (0.002) 0.898 (0.005)	0.085 (0.000) 0.083 (0.000)	0.091 (0.000) 0.091 (0.001)	0.911 (0.003) 0.910 (0.006)	0.091 (0.000) 0.091 (0.000)	0.953 (0.004) 0.954 (0.007)

dominant molecular species) fell from 44 V to 29 V, and in the accelerating voltage experiment, maximum voltages fell from 45 V to 15 V (data not shown). Decreasing the ion source pressure in the MAT 252 also leads to an increase in the relative fragment ion yield and a decrease in the total ion yield. In addition, we note a variation in fragment ion yield in measurements performed with the same gas under ostensibly the same ion source conditions: the relative yield of NO⁺ fragment ions from ¹⁴N¹⁴N¹⁶O measured under normal operating conditions on the Delta Plus XP (i.e. 2.98 kV and 118 eV) varies from 20.951 ± 0.025 in one experiment to 19.357 ± 0.009 in another. We note that the three experiments were performed on three consecutive days, and that gases were loaded fresh each day and scanned for impurities. The variability in relative yield of NO⁺ fragment ions from ¹⁴N¹⁴N¹⁶O between the three days demonstrates the sensitivity of fragment ion formation to small changes in ion source conditions.

In addition to documenting changes in fragmentation rates of a single isotopic species measured under different instrument conditions, Table 2 also shows differences in fragmentation behavior between the four isotopic species tested. These are summarized in Table 3, which shows the fragmentation factors for each isotopically enriched species normalized to the relative yield of NO⁺ ions from ¹⁴N¹⁴N¹⁶O, which is assigned a value of 1. All values are derived from pair-wise comparisons of the tracer gas to UH1-N₂O in manual dual-inlet mode. The most obvious difference is the production of NO⁺ ions by ¹⁵N¹⁵N¹⁶O compared with ¹⁴N¹⁴N¹⁶O: under all experimental conditions, we find c₃₁ to be significantly less than 1 (values range from 0.936 to 0.962). This means that a mixture of ¹⁵N¹⁵N¹⁶O and ¹⁴N¹⁴N¹⁶O will yield a value for ³¹R that is significantly smaller, by around 5%, than ⁴⁶R. The impact of this difference on the calibration of Kaiser *et al.*³⁴ is discussed in the next section.

The difference between ¹⁴N¹⁴N¹⁶O and the mass 45 isotopomers, ¹⁴N¹⁵N¹⁶O and ¹⁵N¹⁴N¹⁶O, is more subtle. The total yield of NO⁺ ions from ¹⁴N¹⁵N¹⁶O is slightly less than the yield from ¹⁴N¹⁴N¹⁶O (i.e. a₃₀ + a₃₁ < 1), and this difference is significant in all instances except for the low-pressure experiment with the MAT 252. ¹⁵N¹⁴N¹⁶O, on the other hand, has a total fragment yield closer to that of ¹⁴N¹⁴N¹⁶O: the sum of b₃₀ and b₃₁ is indistinguishable from 1 in five cases out of eight. Except in the experiment with the Delta Plus XP at fixed accelerating voltage of 3.08 kV, the value of a₃₀ is always significantly less than b₃₁, e.g. 0.088 vs. 0.095 for the Delta Plus XP at normal operating conditions (2.98 kV and 118 eV), and 0.082 vs. 0.091 for the MAT 252, averaged for the high- and low-pressure experiments. This violates the assumption of Kaiser *et al.*³⁴ and Toyoda and Yoshida,¹¹ that the rearrangement or scrambling that takes place in the ion source is symmetric for ¹⁴N¹⁵N¹⁶O and ¹⁵N¹⁴N¹⁶O. We demonstrate this by calculating γ^α and γ^β, the rearrangement coefficients calculated following Kaiser *et al.*: γ^α is the ratio of m/z 30 fragment ions to total fragment ions produced from ¹⁴N¹⁵N¹⁶O and γ^β is the ratio of m/z 31 fragment ions to total fragments produced from ¹⁵N¹⁴N¹⁶O. Except in the case of the Delta Plus XP with a fixed accelerating voltage of

3.08 kV, γ^α is always less than γ^β. This indicates that ¹⁵N¹⁴N¹⁶O molecules show a greater tendency to undergo rearrangement in the ion source than do ¹⁴N¹⁵N¹⁶O molecules.

δ¹⁵N^{bulk} and δ¹⁸O: offline conversion of N₂O into CO₂ and N₂

The combined results of our calibrations of δ¹⁵N^{bulk} and δ¹⁸O by offline conversion into N₂ and CO₂ are summarized in Table 4, along with results of the intercalibration exercises with the laboratories of Thomas Röckmann (Max Planck Institute for Nuclear Physics, Heidelberg, Germany) and Naohiro Yoshida (Tokyo Institute of Technology, Yokohama, Japan). We also include results from our attempts to replicate the tracer addition calibration of Kaiser *et al.*³⁴ and the ammonium nitrate thermal decomposition approach of Toyoda and Yoshida,¹¹ which are discussed in the two sections that follow. Our offline chemical conversion of UH1-N₂O into N₂ and CO₂ yields δ¹⁵N^{bulk} and δ¹⁸O values of 1.53 ± 0.10‰ (mean and standard deviation of 13 runs) vs. air N₂ and 42.30 ± 0.35‰ (mean and standard deviation of 5 runs) vs. VSMOW, respectively. Both values compare favorably with those provided by the Max Planck Institute for Nuclear Physics (1.36‰ and 41.71‰ for two of the aliquots of UH1-N₂O and 1.39‰ and 41.78‰ for three more aliquots of UH1-N₂O: we assume that the difference in these values is due to imperfect gas transfer into the Pyrex tubes) and the Tokyo Institute of Technology (mean values 1.89‰ and 42.07‰ for six aliquots of UH1-N₂O). We therefore accept our δ¹⁵N^{bulk} and δ¹⁸O values for UH1-N₂O and use these values in our subsequent calculations for the isotopomer ratios of UH1-N₂O.

Calibration by tracer addition

Kaiser *et al.*³⁴ performed a position-dependent ¹⁵N calibration of their reference gas using trace additions of ¹⁵N¹⁵N¹⁶O and tracking the increase in ⁴⁶R and ³¹R in the tracer-enhanced gas compared with unadulterated reference gas. The isotope ratios of the tracer-enhanced gas are described as follows:

$$\begin{aligned} {}^{46}\text{R} &= ({}^{15}\text{R}_{\text{ref}}^{\alpha} + {}^{15}\text{R}_{\text{ref}}^{\beta}) {}^{17}\text{R}_{\text{ref}} + {}^{18}\text{R}_{\text{ref}} + {}^{15}\text{R}_{\text{ref}}^{\alpha} \cdot {}^{15}\text{R}_{\text{ref}}^{\beta} \\ &\quad + {}^{15}\text{R}_{1+2} \\ &= {}^{46}\text{R}_{\text{ref}} + {}^{15}\text{R}_{1+2} \end{aligned} \quad (11)$$

$$\begin{aligned} {}^{31}\text{R} &= \frac{\gamma {}^{15}\text{R}_{\text{ref}}^{\alpha} + (1 - \gamma) {}^{15}\text{R}_{\text{ref}}^{\beta} + {}^{15}\text{R}_{\text{ref}}^{\alpha} \cdot {}^{15}\text{R}_{\text{ref}}^{\beta} + {}^{15}\text{R}_{1+2}}{1 + \gamma {}^{15}\text{R}_{\text{ref}}^{\beta} + (1 - \gamma) {}^{15}\text{R}_{\text{ref}}^{\alpha}} \\ &\quad + {}^{17}\text{R} \end{aligned} \quad (12)$$

The term ¹⁵R₁₊₂ represents the ratio of the added tracer with respect to ¹⁴N₂O in the reference gas, and the R_{ref} terms describe the isotope ratios in the reference gas. ¹⁵N¹⁵N¹⁶O tracer was chosen to avoid the complication of rearrangement or scrambling, since only m/z 31 NO⁺ fragment ions can be formed. Comparing aliquots of unadulterated and tracer-enhanced reference gas in dual-inlet measurement mode, Kaiser *et al.*³⁴ define the following

Table 4. Summary of the calibration exercises carried out with UH1-N₂O. The laboratories participating in this exercise were the University of Hawaii, Honolulu, HI, USA (UH), the Max Planck Institute for Nuclear Physics, Heidelberg, Germany (MPI), and the Tokyo Institute of Technology, Yokohama, Japan (TITech)

Laboratory	Calibration approach	$\delta^{15}\text{N}^{\text{bulk}}$ (‰ vs. air N ₂)	$\delta^{15}\text{N}^{\alpha}$ (‰ vs. air N ₂)	$\delta^{15}\text{N}^{\beta}$ (‰ vs. air N ₂)	$\delta^{18}\text{O}$ (‰ vs. VSMOW)	Site preference (‰ vs. air N ₂)
UH	Offline conversion into N ₂ and CO	1.53 ± 0.10			42.30 ± 0.35	
MPI	Dual-inlet measurement against reference gas calibrated by addition of tracer ¹⁵ N ¹⁵ N ¹⁶ O	1.36 ± 0.09	15.60 ± 0.36	-12.88 ± 0.36	41.71 ± 0.20	28.48 ± 0.51
TITech	Dual-inlet measurement against reference gas calibrated by N ₂ O synthesis from NH ₄ NO ₃	1.39 ± 0.09	15.66 ± 0.36	-12.88 ± 0.36	41.78 ± 0.20	28.53 ± 0.51
UH	Addition of tracer ¹⁵ N ¹⁵ N ¹⁶ O following Kaiser <i>et al.</i> ³⁴	1.89 ± 0.4	3.01 ± 0.4	0.77 ± 0.8	42.07 ± 1.2	2.24 ± 0.89
UH	Addition of tracer ¹⁵ N ¹⁵ N ¹⁶ O following Kaiser <i>et al.</i> , ³⁴ corrected for impurities and ¹⁵ N ₂ ⁺		79 ± 1	-76 ± 1		155 ± 1.4
UH	Synthesis of N ₂ O from NH ₄ NO ₃ calculated using a ₃₁ , b ₃₁ and c ₃₁ from mass spectra		84 ± 1	-81 ± 1		165 ± 1.4
UH	Synthesis of N ₂ O from NH ₄ NO ₃ calculated using a single rearrangement coefficient		2.82 ± 0.92	0.25 ± 0.92		2.58 ± 1.85
UH	Synthesis of N ₂ O from NH ₄ NO ₃ calculated using a ₃₁ , b ₃₁ and c ₃₁ from tracer addition		2.83 ± 0.91	0.24 ± 0.91		2.60 ± 1.82
UH	Synthesis of N ₂ O from NH ₄ NO ₃ calculated using a ₃₁ , b ₃₁ and c ₃₁ from tracer addition		2.75 ± 0.85	0.32 ± 0.85		2.44 ± 1.70

ratios:

$${}^{46}\delta = \frac{{}^{46}\text{R}}{{}^{46}\text{R}_{\text{ref}}} - 1 = \frac{{}^{15}\text{R}_{1+2}}{{}^{46}\text{R}_{\text{ref}}} \quad (13)$$

$${}^{31}\delta = \frac{{}^{31}\text{R}}{{}^{31}\text{R}_{\text{ref}}} - 1 = \frac{{}^{15}\text{R}_{1+2}}{{}^{31}\text{R}_{\text{ref}}(1 + \gamma {}^{15}\text{R}_{\text{ref}}^{\beta} + (1 - \gamma){}^{15}\text{R}_{\text{ref}}^{\alpha})} \quad (14)$$

Combining Eqns. (13) and (14) by eliminating the common term ¹⁵R₁₊₂ yields:

$${}^{31}\delta = \frac{{}^{46}\text{R}_{\text{ref}} {}^{46}\delta}{{}^{31}\text{R}_{\text{ref}}(1 + \gamma {}^{15}\text{R}_{\text{ref}}^{\beta} + (1 - \gamma){}^{15}\text{R}_{\text{ref}}^{\alpha})} \quad (15)$$

According to Kaiser *et al.*,³⁴ plotting measured values of ³¹δ vs. ⁴⁶δ should yield a straight line with a slope described by ⁴⁶R_{ref}/³¹R_{ref}[1 + γ¹⁵R_{ref}^β + (1 - γ)¹⁵R_{ref}^α], which can be used, along with Eqn. (9), to derive values for ¹⁵R^α and ¹⁵R^β, as long as ⁴⁶R_{ref}, ¹⁷R and ¹⁵R^{bulk} are known.

We implemented this approach on our ThermoFinnigan Delta Plus XP at an accelerating potential of 2.981 kV using ICON-¹⁵N¹⁵N¹⁶O as our tracer and UH1-N₂O as our base gas. We also repeated the experiment with ICON-¹⁴N¹⁵N¹⁶O and ICON-¹⁵N¹⁴N¹⁶O as tracers. Results are shown in Figs. 1 and 2. Figure 1 shows the response of ³¹δ to increasing ⁴⁶δ following tracer addition of ICON-¹⁵N¹⁵N¹⁶O, the slope of which is the basis for the calibration scheme of Kaiser *et al.*³⁴ Figure 2 shows the response of ³¹δ to increasing ⁴⁵δ following the tracer addition of ICON-¹⁴N¹⁵N¹⁶O and, in a separate mixing series, ICON-¹⁵N¹⁴N¹⁶O. We include this figure to demonstrate the impact of rearrangement or scrambling on measurements of ³¹δ. The measured slope of ³¹δ vs. ⁴⁶δ following ICON-¹⁵N¹⁵N¹⁶O addition is 0.488 (R² = 1). Using an estimated rearrangement factor of 0.088 (γ^α from Table 2, Delta Plus XP at 2.981 kV), and our values for ⁴⁶R_{ref}, ¹⁷R_{ref} and ¹⁵R^{bulk} from calibrating by offline conversion into CO₂ and N₂, we calculate, using Eqn. (15), that δ¹⁵N^α is 79‰ vs. air N₂ and δ¹⁵N^β is -76‰ vs. air N₂. Kaiser *et al.*³⁴ present a

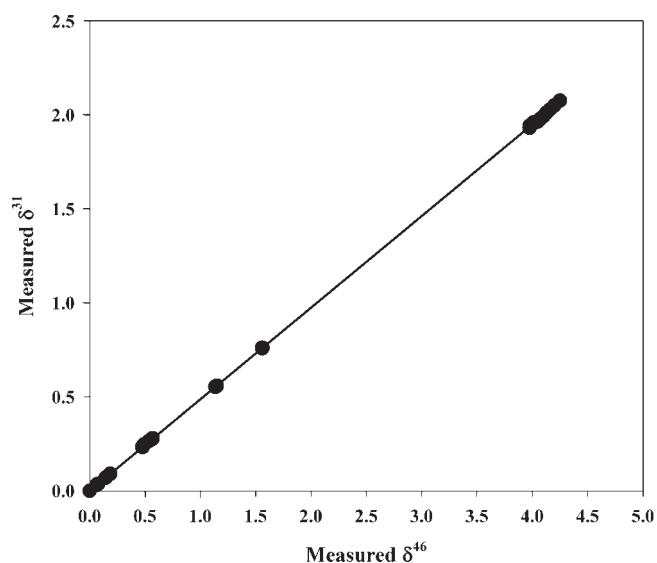


Figure 1. The response of ³¹δ (³¹R/³¹R_{ref} - 1) to ⁴⁶δ (⁴⁶R/⁴⁶R_{ref} - 1) following the addition of trace amounts of ¹⁵N¹⁵N¹⁶O to our reference gas, UH1-N₂O. The relationship can be described by a straight line: y = 0.4876x + 0.0005 (R² = 1).

method for correcting for impurities in the $^{15}\text{N}^{15}\text{N}^{16}\text{O}$ tracer and for the contribution of $^{15}\text{N}^{15}\text{N}^+$ ions from the tracer to m/z 30. These corrections change our values to 84% vs. air N_2 and -81% vs. air N_2 for $\delta^{15}\text{N}^\alpha$ and $\delta^{15}\text{N}^\beta$, respectively. These results are summarized in Table 4, along with measurements of $\text{UH1-N}_2\text{O}$ performed at the Max Planck Institute for Nuclear Physics in Heidelberg, Germany, and the Tokyo Institute of Technology, in Yokohama, Japan. Comparing our

$$^{31}\text{R} = \frac{a_{31}^{15}\text{R}_{\text{ref}}^\alpha + b_{31}^{15}\text{R}_{\text{ref}}^\beta + c_{31}({}^{15}\text{R}_{\text{ref}}^\alpha \cdot {}^{15}\text{R}_{\text{ref}}^\beta + \text{R}_{1+2}) + {}^{17}\text{R}_{\text{ref}}(d_{31} + e_{31}^{15}\text{R}_{\text{ref}}^\alpha + f_{31}^{15}\text{R}_{\text{ref}}^\beta)}{1 + a_{30}^{15}\text{R}_{\text{ref}}^\alpha + b_{30}^{15}\text{R}_{\text{ref}}^\beta + c_{30}({}^{15}\text{R}_{\text{ref}}^\alpha \cdot {}^{15}\text{R}_{\text{ref}}^\beta + \text{R}_{1+2})} \quad (16)$$

values for $\delta^{15}\text{N}^\alpha$ and $\delta^{15}\text{N}^\beta$ (84% and -81%) with those generated in Heidelberg (15.6% and -12.9%) and Yokohama (3.0% and 0.8%), we do not find this calibration exercise to have yielded credible results.

The calibration approach advocated by Kaiser *et al.*³⁴ rests on the assumption that tracers behave in an equivalent manner among molecular ions and fragment ions. This assumption is expressed in the use of a single term, $^{15}\text{R}_{1+2}$, to describe the effect of the addition of a tracer to the molecular ion ratio, ^{46}R , and the fragment ion ratio, ^{31}R . The work of Begun and Landau,³⁶ and our measurements of the fragmentation patterns of $^{14}\text{N}^{15}\text{N}^{16}\text{O}$, $^{15}\text{N}^{14}\text{N}^{16}\text{O}$ and $^{15}\text{N}^{15}\text{N}^{16}\text{O}$ compared with that of $^{14}\text{N}^{14}\text{N}^{16}\text{O}$, show that this assumption is incorrect and that different isotopic species form fragments at different rates, determined both by their molecular characteristics (such as bond strength and zero point energy) and by conditions in the ion source of the mass spectrometer used for the measurement. We note that, in all our measurements, the relative yield of $^{15}\text{N}^{16}\text{O}^+$ from $^{15}\text{N}^{15}\text{N}^{16}\text{O}$ is lower than the relative yield of $^{14}\text{N}^{16}\text{O}^+$ from

$^{14}\text{N}^{14}\text{N}^{16}\text{O}$, by around 5% (see the values of c_{31} listed in Table 3).

Taking into account possible isotope effects of fragment ion formation, we have the following relationships for the trace addition of $\text{UH1-N}_2\text{O}$ to our reference gas, $\text{UH1-N}_2\text{O}$:

$$^{46}\text{R} = ^{46}\text{R}_{\text{ref}} + \text{R}_{1+2} \quad (11)$$

Focusing on the response to tracer addition, we define:

$$^{31}\text{R}_{\text{ref}} = \frac{x_{31}}{x_{30}} \quad (17)$$

It follows that:

$$^{31}\text{R} = \frac{x_{31} + c_{31}\text{R}_{1+2}}{x_{30} + c_{30}\text{R}_{1+2}} \quad (18)$$

As we know $^{46}\text{R}_{\text{ref}}$, we can use the measured ion ratios, or 'raw' ratios, of ^{46}R and $^{46}\text{R}_{\text{ref}}$ to calculate R_{1+2} for any given gas mixture:

$$\text{R}_{1+2} = ^{46}\text{R}_{\text{ref}} \left(\frac{^{46}\text{R}}{^{46}\text{R}_{\text{ref}}} - 1 \right) \quad (19)$$

Comparing measured fragment ion ratios, we have:

$$\frac{^{31}\text{R}}{^{31}\text{R}_{\text{ref}}} = \frac{\frac{x_{31} + c_{31}\text{R}_{1+2}}{x_{30} + c_{30}\text{R}_{1+2}}}{\frac{x_{31}}{x_{30}}} \quad (20)$$

The response of the fragment ion signal ratio to tracer addition takes the form:

$$\frac{^{31}\text{R}}{^{31}\text{R}_{\text{ref}}} = \frac{1 + z_{31}\text{R}_{1+2}}{1 + z_{30}\text{R}_{1+2}} \quad (21)$$

The terms z_{31} and z_{30} are c_{31}/x_{31} and c_{30}/x_{30} , respectively. Since we can calculate R_{1+2} and measure $^{31}\text{R}/^{31}\text{R}_{\text{ref}}$, we can obtain values for z_{31} and z_{30} by nonlinear regression to the curve formed as the ratio $^{31}\text{R}/^{31}\text{R}_{\text{ref}}$ responds to R_{1+2} . Because z_{31} and z_{30} contain the constants c_{31} and c_{30} , our estimates of x_{31} and x_{30} , from which we derive $^{15}\text{R}^\alpha$ and $^{15}\text{R}^\beta$, can only be as accurate as our knowledge of the isotope effects associated with fragment ion formation. The response of the fragment ion ratio to tracer enrichments of $^{14}\text{N}^{15}\text{N}^{16}\text{O}$ or $^{15}\text{N}^{14}\text{N}^{16}\text{O}$ will take the identical form, with the constants c_{31} and c_{30} replaced by a_{31} and a_{30} and b_{31} and b_{30} , respectively. Therefore, we see that any attempt to calibrate a laboratory reference gas by tracer addition requires detailed knowledge of the fragmentation behavior of nitrous oxide within a given set of ion source conditions.

To demonstrate the vulnerability of a calibration performed by tracer addition to isotope effects associated with fragmentation, we return to the approach of Kaiser *et al.*³⁴ and consider the relationship between $^{46}\delta$ and $^{31}\delta$ in the limit

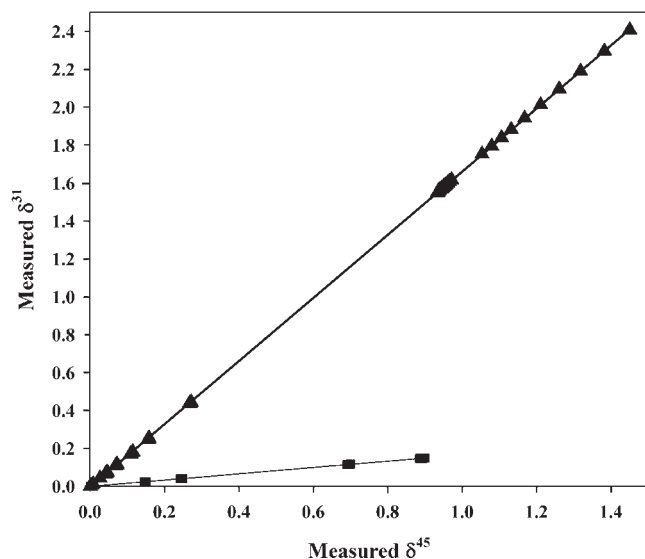


Figure 2. The response of $^{31}\delta$ ($^{31}\text{R}/^{31}\text{R}_{\text{ref}} - 1$) to $^{45}\delta$ ($^{45}\text{R}/^{45}\text{R}_{\text{ref}} - 1$) following the addition of trace amounts of $^{14}\text{N}^{15}\text{N}^{16}\text{O}$ (\blacktriangle) and $^{15}\text{N}^{14}\text{N}^{16}\text{O}$ (\blacksquare) to our reference gas, $\text{UH1-N}_2\text{O}$. The responses are well described by straight lines: addition of $^{14}\text{N}^{15}\text{N}^{16}\text{O}$ yields $^{31}\delta = 1.665^{45}\delta - 0.004$ ($R^2 = 1$) and addition of $^{15}\text{N}^{14}\text{N}^{16}\text{O}$ yields $^{31}\delta = 0.1660^{45}\delta - 0.0002$ ($R^2 = 1$).

of low tracer addition:

$${}^{46}\delta = \frac{{}^{46}\text{R}}{{}^{46}\text{R}_{\text{ref}}} - 1 = \frac{{}^{15}\text{R}_{1+2}}{{}^{46}\text{R}_{\text{ref}}} \quad (13)$$

$${}^{31}\delta = \frac{{}^{31}\text{R}}{{}^{31}\text{R}_{\text{ref}}} - 1 = \frac{1 + z_{31}{}^{15}\text{R}_{1+2}}{1 + z_{30}{}^{15}\text{R}_{1+2}} - 1 \quad (22)$$

Substituting for ${}^{15}\text{R}_{1+2}$ using Eqn. (13), we obtain:

$${}^{31}\delta = \frac{1 + z_{31}{}^{46}\text{R}_{\text{ref}}{}^{46}\delta}{1 + z_{30}{}^{46}\text{R}_{\text{ref}}{}^{46}\delta} - 1 \quad (23)$$

Using a Maclaurin series to expand ${}^{31}\delta$ as a function of ${}^{46}\delta$ about the point ${}^{46}\delta = 0$, the coefficient of the linear term is: $(z_{31} - z_{30}){}^{46}\text{R}_{\text{ref}}$, or:

$$\text{Slope} = \left[\frac{c_{31}}{x_{31}} - \frac{c_{30}}{x_{30}} \right] {}^{46}\text{R}_{\text{ref}} \quad (24)$$

Substituting ${}^{31}\text{R}_{\text{ref}}x_{30}$ for x_{31} (from Eqn. (17)), and writing x_{30} explicitly, yields:

$$\text{Slope} = \left[\frac{c_{31} - c_{30}{}^{31}\text{R}_{\text{ref}}}{{}^{31}\text{R}_{\text{ref}}(1 + a_{30}{}^{15}\text{R}^{\alpha} + b_{30}{}^{15}\text{R}^{\beta} + c_{30}{}^{15}\text{R}^{\alpha} \cdot {}^{15}\text{R}^{\beta})} \right] {}^{46}\text{R}_{\text{ref}} \quad (25)$$

Apart from differences in how we treat 'scrambling', this is identical to the expression derived by Kaiser *et al.*³⁴ for the slope of the line formed when we plot ${}^{31}\delta$ as a function of ${}^{46}\delta$ with one important exception: we do not assume that c_{31} , the ratio of the yield of ${}^{15}\text{N}^{16}\text{O}^+$ ions from ${}^{15}\text{N}^{15}\text{N}^{16}\text{O}$ relative to the yield of ${}^{14}\text{N}^{16}\text{O}^+$ ions from ${}^{14}\text{N}^{14}\text{N}^{16}\text{O}$, has a value of 1. Since ${}^{31}\text{R}_{\text{ref}}$ is likely to be small (on the order of 0.004), we see that c_{31} is by far the dominant term in the numerator of this expression. The position-dependent ${}^{15}\text{N}$ calibration published by Kaiser *et al.*³⁴ is derived by fitting values for ${}^{15}\text{R}^{\alpha}$ and ${}^{15}\text{R}^{\beta}$ to an expression for the slope of the line formed between ${}^{31}\delta$ and ${}^{46}\delta$ as ${}^{15}\text{N}^{15}\text{N}^{16}\text{O}$ tracer gas is added to the reference gas. If we include in our expression for this slope all the possible isotope effects associated with fragment ion formation (as shown in Eqn. (25)), we can estimate the impact of any deviation of the value of c_{31} from 1 by simply allowing c_{31} to vary and calculating the ${}^{15}\text{R}^{\alpha}$ and ${}^{15}\text{R}^{\beta}$ values that yield a fit to our measured slope of 0.488. Figure 3 shows the response of the calculated ${}^{15}\text{N}$ site preference ($\text{SP} = \delta^{15}\text{N}^{\alpha} - \delta^{15}\text{N}^{\beta}$) from our measured slope value of 0.488 as we allow c_{31} to vary from 0.9 to 1. The response is both linear and strong (by linear fit, $\text{SP} = 2898c_{31} - 2741$, $R^2 = 1$), such that a small difference in c_{31} (e.g. ± 0.01 , or $\pm 1\%$) leads to a large difference in calculated site preference ($\pm 29\%$). Similar relationships can be demonstrated for the other two tracers: varying a_{31} in the calculation of the slope between ${}^{31}\delta$ and ${}^{45}\delta$ following ${}^{14}\text{N}^{15}\text{N}^{16}\text{O}$ addition leads to $\text{SP} = 3216 a_{31} - 2743$ and varying b_{31} following ${}^{15}\text{N}^{14}\text{N}^{16}\text{O}$ addition leads to $\text{SP} = 29920b_{31} - 2740$.

We reject tracer mixing as a means to calibrate the site preference of an unknown reference gas on the basis of the extreme sensitivity of calculated site preference to small changes in the relative yield of m/z 31 ions from the tracer gases. We do not believe that a simple examination of the mass spectra of purified tracer gases can yield the constants a_{31} , b_{31} and c_{31} to sufficient precision to allow for an accurate calculation of the site preference of an unknown reference gas from mixing curves generated by

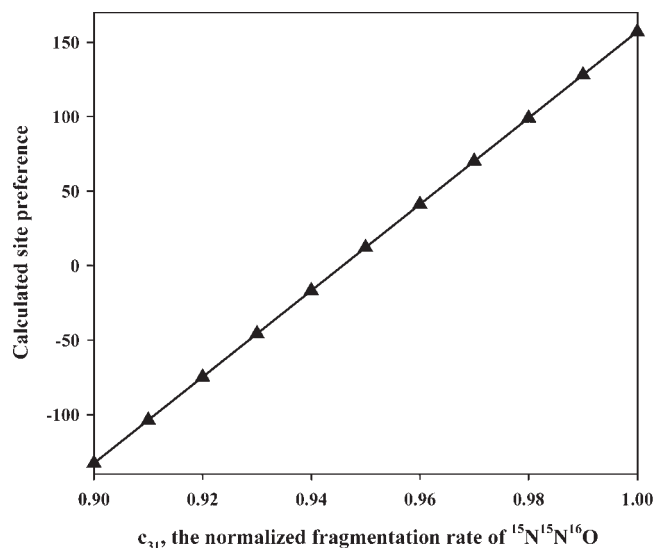


Figure 3. The response of calculated site preference ($\text{SP} = \delta^{15}\text{N}^{\alpha} - \delta^{15}\text{N}^{\beta}$) to changes in c_{31} , the rate of ${}^{15}\text{N}^{16}\text{O}^+$ formation from ${}^{15}\text{N}^{15}\text{N}^{16}\text{O}$ normalized to the rate of ${}^{14}\text{N}^{16}\text{O}^+$ from ${}^{14}\text{N}^{14}\text{N}^{16}\text{O}$, based on the measured slope of the response of ${}^{31}\delta$ to ${}^{46}\delta$ following trace addition of ${}^{15}\text{N}^{15}\text{N}^{16}\text{O}$ to our reference gas, UH1-N₂O. This calculation is the basis for the Kaiser *et al.*³⁴ calibration, which assumes that c_{31} is 1.

tracer addition of ${}^{14}\text{N}^{15}\text{N}^{16}\text{O}$, ${}^{15}\text{N}^{14}\text{N}^{16}\text{O}$ or ${}^{15}\text{N}^{15}\text{N}^{16}\text{O}$. The converse, however, may be useful: given knowledge of the ${}^{15}\text{N}$ site preference of a reference gas, tracer mixing curves can be used to evaluate a_{31} , b_{31} and c_{31} under a given set of measurement conditions. This is essentially the approach taken by Toyoda and Yoshida¹¹ and Röckmann *et al.*¹⁵ to evaluate γ , the 'rearrangement fraction', defined as 'the fraction of NO⁺ bearing β nitrogen of the initial N₂O to the total NO⁺ formed'. We note that their γ value is equivalent to our value b_{31} .

Calibration by synthesis of N₂O from ammonium nitrate

Using the method described in Toyoda and Yoshida¹¹ modified with a higher reaction temperature and shorter reaction time, we converted five isotopically distinct samples of NH₄NO₃ into N₂O and N₂ by thermal decomposition. One sample was unadulterated, three had added ${}^{15}\text{NO}_3^-$ and one had added ${}^{15}\text{NH}_4^+$. Table 5 summarizes the results of the thermal decomposition of these samples, as well as measurements of the bulk $\delta^{15}\text{N}$ values of the NH₄NO₃ starting material and the $\delta^{15}\text{N}$ values of the NH₄⁺ fraction. We find complete thermal decomposition after 1 h of heating, but the relative yield of N₂ gas from Reaction 2 is higher than expected: Brower *et al.*⁴¹ report a 6% yield of N₂ for samples reacted above 300°C, but we find N₂ yields ranging from 21.9% to 35.3%. With such a high proportion of unwanted product, the potential for fractionation caused by divergence in the isotope effects of the two competing reactions ($\text{NH}_4\text{NO}_3 \rightarrow \text{N}_2\text{O} + 2\text{H}_2\text{O}$ vs. $5\text{NH}_4\text{NO}_3 \rightarrow 4\text{N}_2 + 9\text{H}_2\text{O} + 2\text{HNO}_3$) could be large. However, Fig. 4, a plot of $\delta^{15}\text{N}_2\text{O}^{\text{bulk}}$ and $\delta^{15}\text{N}_2$ as a function of the $\delta^{15}\text{N}$ value of the starting

Table 5. Results of the isotopomer calibration of UH1-N₂O by comparison to N₂O samples synthesized by thermal decomposition of isotopically characterized NH₄NO₃, as described in the text

Measured values for NH ₄ NO ₃				Measured values for N ₂ O and N ₂ from NH ₄ NO ₃			Resulting values for UH1-N ₂ O			
Preparation	$\delta^{15}\text{N-NH}_4\text{NO}_3$	$\delta^{15}\text{N-NH}_4^+$	% yield N ₂ O	$\delta^{15}\text{N}_2\text{O}$	$\delta^{18}\text{N}_2\text{O}$	% yield N ₂	$\delta^{15}\text{N}_2$	$\delta^{15}\text{N}^\alpha$	$\delta^{15}\text{N}^\beta$	¹⁵ N site preference
Recrystallized NH ₄ NO ₃	-1.14 ± 0.12	-1.11 ± 0.04	73.66	-0.75	37.33	22.64	0.75	3.86	-0.79	4.65
			66.25	-0.73	37.06	28.54	1.85	3.28	-0.21	3.48
			65.65	-1.13	37.37	28.16	1.32	1.62	1.45	0.17
			69.46	-0.81	37.78	25.32	1.68	2.21	0.86	1.35
			64.43	-1.31	37.68	29.43	0.64	2.18	0.89	1.29
NH ₄ NO ₃ + low ¹⁵ NO ₃	5.15 ± 0.32	-0.85 ± 0.08	58.81	4.46	38.85	34.18	5.05	2.75	0.32	2.44
			61.49	4.33	38.15	32.06	4.40	3.51	-0.44	3.94
NH ₄ NO ₃ + mid ¹⁵ NO ₃	8.43 ± 0.09	-1.11 ± 0.04	65.57	8.06	39.68	28.96	9.41	4.16	-1.09	5.25
			64.25	7.90	39.80	29.27	9.42	3.42	-0.35	3.76
			65.47	7.80	39.48	28.76	9.44	3.45	-0.38	3.83
			66.07	7.71	39.51	29.58	9.38	3.33	-0.26	3.59
			60.83	7.71	39.51	32.65	9.29	2.47	0.60	1.87
NH ₄ NO ₃ + high ¹⁵ NO ₃	13.25 ± 0.20	-0.96 ± 0.17	62.56	12.35	36.65	35.26	12.49	2.41	0.66	1.74
			55.16	12.05	36.24	34.72	12.61	3.21	-0.14	3.36
			58.80	12.95	37.71	33.28	13.01	4.91	-1.84	6.75
NHNO ₃ + ¹⁵ NH ₄	11.61 ± 0.15	21.93 ± 0.03	66.33	10.43	37.13	28.99	14.20	1.20	1.87	-0.67
			73.70	10.96	38.40	29.65	14.68	2.07	1.00	1.07
			73.19	10.23	35.55	24.00	15.14	1.94	1.13	0.81
			69.34	10.26	36.75	25.10	14.22	2.17	0.90	1.27
			71.88	10.34	36.15	21.88	15.18	2.35	0.72	1.63

material, shows that the isotope effects associated with N₂O production from NH₄NO₃ are relatively small and appear to be symmetrically distributed between the two nitrogen positions. We include $\delta^{15}\text{N}_2$ values on this chart, which, although somewhat variable, serve to demonstrate that the isotope effect of Reaction 2 is also small, and has the opposite direction of the isotope effect of Reaction 1, so that

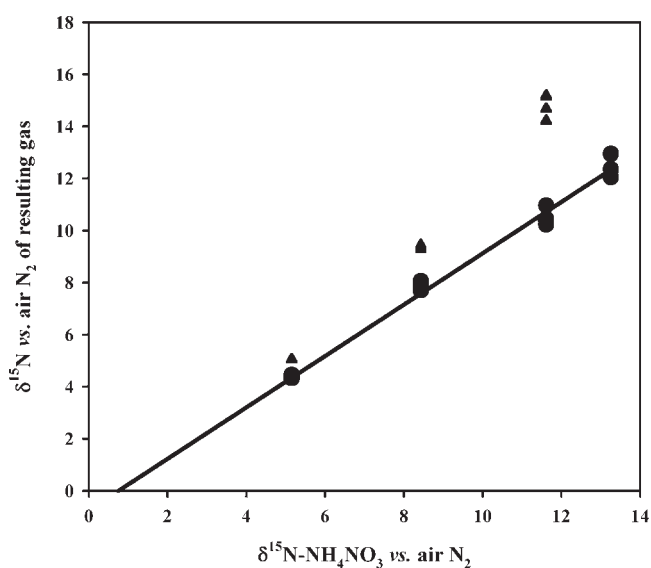


Figure 4. Isotope effects associated with the thermal decomposition of NH₄NO₃ to N₂O (●) and N₂ (▲). The relationship between $\delta^{15}\text{N}_2\text{O}^{\text{bulk}}$ and $\delta^{15}\text{N-NH}_4\text{NO}_3$ can be described by a straight line with slope 0.987 and intercept -0.736 ($R^2 = 0.996$).

all ¹⁵N in the starting NH₄NO₃ is essentially accounted for in the resulting N₂O and N₂. The relationship between $\delta^{15}\text{N}_2\text{O}^{\text{bulk}}$ and $\delta^{15}\text{N-NH}_4\text{NO}_3$ is well described by a straight line with a slope near 1 and a small offset at the y-axis: $y = 0.992x - 0.793$, $R^2 = 0.996$. The one set of samples that were labeled with ¹⁵NH₄⁺, presumably yielding N₂O enriched in ¹⁵N^β, lie on the same linear trend as three sets of samples labeled with varying amounts of ¹⁵NO₃⁻, yielding N₂O enriched in ¹⁵N^α. Therefore, we estimate $\delta^{15}\text{N}_2\text{O}^\beta$ for our synthesized gases from the measured $\delta^{15}\text{N}$ value of the constituent ammonium corrected according to the relationship $\delta^{15}\text{N}_2\text{O}^\beta = 0.992 \times \delta^{15}\text{N-NH}_4^+ - 0.793$ (see Fig. 4). We calculate $\delta^{15}\text{N}_2\text{O}^\alpha$ as $2 \times \delta^{15}\text{N}_2\text{O}^{\text{bulk}} - \delta^{15}\text{N}_2\text{O}^\beta$.

With ¹⁸R, ¹⁷R and ¹⁵R^{bulk} derived from comparison with UH1-N₂O and $\delta^{15}\text{N}_2\text{O}^\beta$ from knowledge of the starting $\delta^{15}\text{N-NH}_4^+$ of NH₄NO₃ and the measured isotope effect associated with thermal decomposition, we now have enough information to use our synthesized gases to perform a position-dependent calibration of our laboratory reference gas. We use Eqn. (10) and our measured fragmentation factors (a_{30} , a_{31} , b_{30} , b_{31} , c_{30} and c_{31} , from Table 3; we assume d_{31} is 1 since we cannot quantify it directly but we know that the contribution of ¹⁷R to ³¹R is very small) to calculate a value for ³¹R for each synthesized gas. We use this value to convert the measured (or 'raw') ratio of m/z 31 to m/z 30 for UH1-N₂O into a measured ³¹R value, then iterate ¹⁵R^α of UH1-N₂O until the calculated ³¹R value is equal to the measured ³¹R value (see Table 5).

Based on measurements of 20 synthesized N₂O samples from five isotopically distinct batches of NH₄NO₃, our values for $\delta^{15}\text{N}^\alpha$ and $\delta^{15}\text{N}^\beta$ of our laboratory reference gas, UH1-N₂O, are 2.82‰ and 0.25‰ vs. air N₂, respectively,

each with SDs of 0.92%. These values are essentially indistinguishable from those provided for UH1-N₂O by the Tokyo Institute of Technology in Yokohama, Japan (3.01% and 0.77%). They diverge significantly from those provided by the Max Planck Institute for Nuclear Physics, in Heidelberg, Germany (15.63% and -12.88%), and are very different from the results of our own tracer calibration exercise (84% and -81%, with corrections for impurities; see Table 5). It appears that the NH₄NO₃ approach, while laborious and somewhat imprecise, is nevertheless accurate: compared with Toyoda and Yoshida,¹¹ we use different reaction times and temperatures for thermal decomposition, we make our measurements on a different model of mass spectrometer, and we approach the isotopomer calculations from a different theoretical perspective, and yet our results converge. We also note that this approach is not very sensitive to differences in the calculation scheme for ³¹R: when we reanalyze the results from our NH₄NO₃ experiment using the approach described in Toyoda and Yoshida,¹¹ which includes a single fragmentation factor, γ (we use the average of our measured values for γ^α and γ^β), we find that our values for $\delta^{15}\text{N}^\alpha$ and $\delta^{15}\text{N}^\beta$ differ only in the second decimal place, a difference that is negligible for most real-world applications of N₂O isotopomer analysis. We therefore support the acceptance of the isotopomer calibration of Toyoda and Yoshida¹¹ as the current community standard and reject the tracer addition calibration method proposed by Kaiser *et al.*³⁴

Combining calibration approaches to refine estimates of fragmentation factors

Because of the great sensitivity of site preference to the fragmentation factors a_{31} , b_{31} and c_{31} , tracer mixing is not a reliable method to calibrate the site preference of an unknown laboratory reference gas. However, the reproducible and robust response of ³¹ δ to tracer addition suggests that this approach could provide a better way to quantify fragmentation factors than simple measurements of the mass spectra of purified tracer gases. Accepting the calibration of Toyoda and Yoshida¹¹ for our reference gas ($\delta^{15}\text{N}^\alpha = 3.01\%$, $\delta^{15}\text{N}^\beta = 0.77\%$, SP = 2.24%, all values vs. air N₂), we can calculate the following values for a_{31} , b_{31} and c_{31} from site preference using the empirical relationships:

$$\text{SP} = 3216a_{31} - 2743, \quad a_{31} = 0.854 \quad (26)$$

$$\text{SP} = 29920b_{31} - 2740, \quad b_{31} = 0.092 \quad (27)$$

$$\text{SP} = 2898c_{31} - 2741, \quad c_{31} = 0.947 \quad (28)$$

We adjust these values for known impurities as follows: for our ICON-¹⁴N¹⁵N¹⁶O and ICON-¹⁵N¹⁴N¹⁶O, we assume a 0.1% contribution of the unwanted mass 45 isotopomer (from Kaiser *et al.*³⁴), such that a_{31} in Eqn. (26) becomes $0.999a_{31} + 0.001b_{31}$ and b_{31} in Eqn. (27) becomes $0.999b_{31} + 0.001a_{31}$. This increases a_{31} to 0.855 and reduces b_{31} to 0.091. From Table 1, we know that 0.93% of

ICON-¹⁵N¹⁵N¹⁶O gas is mass 45, which contributes to the ³¹ δ measurement but not to the ⁴⁶ δ measurement, so our value of c_{31} needs to be adjusted downwards such that c_{31} in Eqn. (28) becomes $c_{31} + 0.0046a_{31} + 0.0046b_{31}$. This reduces our value for c_{31} to 0.942. From this exercise, we see that all of the m/z 31 fragmentation factors are slightly smaller than the same factors calculated from simple comparisons of the tracer gases with UH1-N₂O (a_{31} , b_{31} and c_{31} were 0.904, 0.095 and 0.952, respectively), but we choose these latter values since we believe that the response to low-level tracer enrichment provides a better prediction of how our instrument will respond to natural N₂O samples than do measurements of purified gases. We do not adjust our m/z 30 fragmentation factors (a_{30} , b_{30} and c_{30}) since, for natural abundance measurements, the contribution of ¹⁴N¹⁴N¹⁶O will so dominate the denominator in the expression for ³¹R that small variations in a_{30} , b_{30} and c_{30} should not be detectable. Revising our values for a_{31} , b_{31} and c_{31} in the isotope calibration of UH1-N₂O by comparison with N₂O synthesized from ammonium nitrate yields values of $2.75 \pm 0.85\%$ vs. air N₂ for $\delta^{15}\text{N}^\alpha$ and $0.32 \pm 0.85\%$ vs. air N₂ for $\delta^{15}\text{N}^\beta$, bringing our revised value for site preference, 2.44%, slightly closer to the Tokyo Institute of Technology value of 2.24% (see Table 5). We advocate the use of the tracer mixing approach described in Kaiser *et al.*³⁴ to evaluate a_{31} , b_{31} and c_{31} for IRMS N₂O measurements using a given set of ion source conditions. Those laboratories interested in accurate measurements of the abundance of ¹⁴N¹⁴N¹⁷O are advised to evaluate the constants d_{31} , e_{31} and f_{31} using tracer addition of ¹⁴N¹⁴N¹⁷O.

SUMMARY AND CONCLUSIONS

Distinguishing between the ¹⁵N-substituted isotopomers of N₂O, ¹⁴N¹⁵N¹⁶O and ¹⁵N¹⁴N¹⁶O required a significant innovation in IRMS, the analysis of both molecular and fragment ions generated by electron ionization in the ion source.^{11,12} Two groups simultaneously pioneered this measurement and both recognized that fragment ion analysis is fundamentally different from molecular ion analysis, and observed and quantified the phenomenon of 'scrambling', or molecular rearrangement, that occurs during ionization and leads to the production of ¹⁴N¹⁶O⁺ from ¹⁴N¹⁵N¹⁶O and ¹⁵N¹⁶O⁺ from ¹⁵N¹⁴N¹⁶O. In our effort to replicate the calibration approaches of both groups and identify the source of the current calibration controversy, we came to recognize that 'scrambling' is a specific case of a more general phenomenon: that the different isotopic species of N₂O form NO⁺ fragment ions at different rates, and these rates are affected both by the physical nature of the molecule (e.g. bond strength and zero point energy) and by the specific conditions in the mass spectrometer ion source. We revise the current treatment of isotope calculations to include all possible fragmentation factors, normalized to the rate of formation of ¹⁴N¹⁶O⁺ from ¹⁴N¹⁴N¹⁶O:

$${}^{31}\text{R} = \frac{a_{31}{}^{15}\text{R}^\alpha + b_{31}{}^{15}\text{R}^\beta + c_{31}{}^{15}\text{R}^\alpha \cdot {}^{15}\text{R}^\beta + {}^{17}\text{R}(d_{31} + e_{31}{}^{15}\text{R}^\alpha + f_{31}{}^{15}\text{R}^\beta)}{1 + a_{30}{}^{15}\text{R}^\alpha + b_{30}{}^{15}\text{R}^\beta + c_{30}{}^{15}\text{R}^\alpha \cdot {}^{15}\text{R}^\beta} \quad (16)$$

where the constants a_{31} and a_{30} represent the tendency for $^{14}\text{N}^{15}\text{N}^{16}\text{O}$ to form m/z 31 and m/z 30 fragments, respectively; b_{31} and b_{30} represent the tendency for $^{15}\text{N}^{14}\text{N}^{16}\text{O}$ to form m/z 31 and m/z 30 fragments; c_{31} and c_{30} represent the tendency for $^{15}\text{N}^{15}\text{N}^{16}\text{O}$ to form m/z 31 and m/z 30 fragments (the m/z 30 fragments are $^{15}\text{N}_2^+$ ions); and d_{31} , e_{31} and f_{31} represent the tendencies for ^{17}O -containing isotopologues to form m/z 31 fragments. All constants are normalized to the tendency for $^{14}\text{N}^{14}\text{N}^{16}\text{O}$ to form m/z 30 fragments, to which we assign a value of 1.

The calibration approach of Kaiser *et al.*³⁴ is based on the assumption that $^{15}\text{N}^{15}\text{N}^{16}\text{O}$ forms $^{15}\text{N}^{16}\text{O}^+$ fragment ions at the same rate as $^{14}\text{N}^{14}\text{N}^{16}\text{O}$ forms $^{14}\text{N}^{16}\text{O}^+$ fragment ions, and that the value of c_{31} is always 1. We have shown that this is not the case, that c_{31} is always less than 1, and varies with ion source conditions, so that the calibration of Kaiser *et al.*³⁴ yields different results for the same gas analyzed by different mass spectrometers. We believe that this is the cause of the discrepancy between the calibrations of Kaiser *et al.*³⁴ and Toyoda and Yoshida¹¹ for the ^{15}N site preference of tropospheric N_2O , rather than systematic errors in the absolute isotope ratios of the primary isotopic reference materials air- N_2 and VSMOW, as suggested by Kaiser *et al.*³⁴ For example, the ^{15}N site preference values for UH1- N_2O measured in Yokohama and in Heidelberg are 2.2‰ and 28.5‰, respectively, but when we perform our own calibration using the Kaiser *et al.*³⁴ approach we obtain 165‰, a value that cannot be reconciled with the other two values by making small adjustments to the isotopic ratios of the reference materials. Other laboratories have attempted the calibration with $^{15}\text{N}_2\text{O}$ and have obtained similarly unbelievable results (Sakae Toyoda, Tokyo Institute of Technology, Yokohama, Japan, personal communication, and Karen Casciotti, Woods Hole Oceanographic Institute, MA, USA, personal communication). Thus it seems that it is the method that is at fault, not the reference values.

While the tracer mixing approach advocated by Kaiser *et al.*³⁴ failed to yield an accurate estimate of the ^{15}N site preference of UH1- N_2O , it did yield valuable information on the variable fragmentation rates of the isotopic species of N_2O . We recommend that all laboratories measuring isotopomers of N_2O by IRMS use isotopically enriched tracers ($^{14}\text{N}^{15}\text{N}^{16}\text{O}$, $^{15}\text{N}^{14}\text{N}^{16}\text{O}$ and $^{15}\text{N}^{15}\text{N}^{16}\text{O}$) mixed into a calibrated laboratory reference gas as a means to quantify a_{31} , b_{31} and c_{31} for a specific instrument. The values of a_{30} , b_{30} and c_{30} are not accessible by this technique and thus must be obtained from measurements of fragment ion formation from purified tracer gases. Since fragmentation factors are sensitive to instrument conditions, these exercises should be repeated periodically and certainly following any change in the ion source conditions such as filament replacement.

In contrast to tracer mixing, calibration based on the synthesis of N_2O by thermal decomposition of NH_4NO_3 , while laborious and somewhat imprecise, appears essentially robust. By comparing N_2O synthesized from ammonium nitrate with a range of isotopic compositions, we find that the isotopic effects of thermal

decomposition are small and apparently symmetric. From measurements of 20 synthesized N_2O samples, we derive a ^{15}N site preference value of $2.6 \pm 1.8\%$ for UH1- N_2O , essentially indistinguishable from the value of 2.2‰ provided by the Tokyo Institute of Technology in Yokohama, Japan. We emphasize that we used a higher reaction temperature (360°C compared with 225–230°C), a shorter reaction time (1 hour vs. 4–5 days), a range of isotopic compositions of starting NH_4NO_3 and a different model of mass spectrometer to measure the resulting N_2O . It is possible that performing the thermal decomposition of ammonium nitrate in a vacuum line with continuous removal of product N_2O , following the protocol of Friedman and Bigeleisen,¹⁰ or under a continuous flow of helium following Rosser *et al.*,⁴² will yield a more precise result, but we believe that our measurements, while somewhat crude, provide an important independent verification of the results presented in Toyoda and Yoshida.¹¹ We have no justification for replacing the Japanese calibration with our own, and instead advocate intercalibration with the Tokyo Institute of Technology as the most efficient and reliable standardization method. What is essential is that results be comparable between laboratories and measurements be performed on a common scale. We believe that the N_2O mass spectrometry community should designate a single N_2O standard and establish an efficient mechanism for its maintenance and distribution. Until a third, independent calibration is developed, we support the calibration reported in Toyoda and Yoshida¹¹ as the most accurate basis for a community standard.

Acknowledgements

We thank Sakae Toyoda of the Tokyo Institute of Technology (Yokohama, Japan) for measuring our reference gas, for providing advice during the preparation of this manuscript and for checking our isotope calculations. Thomas Röckmann, now at Utrecht University (Utrecht, The Netherlands), also participated in the intercalibration exercise. Mike Lott of the University of Utah (Salt Lake City, UT, USA) provided the protocol for separating ammonium from ammonium nitrate. Natalie Wallsgrove at the University of Hawaii undertook the separations and Jamie Tanimoto, also at the University of Hawaii, performed the isotopic analyses. Anand Gnanadesikan of the Geophysical Fluids Dynamics Laboratory (Princeton, NJ, USA) and Edward Laws of Louisiana State University (Baton Rouge, LA, USA) provided insightful readings of early drafts of this manuscript. The authors are indebted to John Hayes of the Woods Hole Oceanographic Institute (Woods Hole, MA, USA) and Jacob Bigeleisen of Stony Brook University (Emeritus) (Stony Brook, NY, USA) for pedagogical discussions concerning isotope effects and the nature of mass spectrometry. Finally, we thank two anonymous reviewers and Jan Kaiser of the University of East Anglia (Norwich, UK) for helping us to improve this manuscript. Support for laboratory work was provided by National Science Foundation grant OCE-0240787 to Brian N. Popp. Support for Marian Westley is provided by the National Oceanic and Atmospheric Administration's Educational Partnership Program. This is SOEST Contribution 7012.

REFERENCES

1. Yung YL, Wang WC, Lacis AA. *Geophys. Res. Lett.* 1976; **3**: 619.
2. Crutzen PJ. *Q. J. R. Meteorol. Soc.* 1970; **96**: 320.
3. Kim KR, Craig H. *Science* 1993; **262**: 1855.
4. Pérez T, Trumbore SE, Tyler SC, Davidson EA, Keller M, de Camargo PB. *Global Biogeochem. Cycles* 2000; **14**: 525.
5. Kim KR, Craig H. *Nature* 1990; **347**: 58.
6. Dore JE, Popp BN, Karl DM, Sansone FJ. *Nature* 1998; **396**: 63.
7. Naqvi SWA, Yoshinari T, Jayakumar DA, Altabet MA, Narvekar PV, Devol AH, Brandes JA, Codispoti LA. *Nature* 1998; **394**: 462.
8. Rahn T, Wahlen M. *Science* 1997; **278**: 1776.
9. Yung YL, Miller CE. *Science* 1997; **278**: 1778.
10. Friedman L, Bigeleisen J. *J. Chem. Phys.* 1950; **18**: 1325.
11. Toyoda S, Yoshida N. *Anal. Chem.* 1999; **71**: 4711.
12. Brenninkmeijer CAM, Röckmann T. *Rapid Commun. Mass Spectrom.* 1999; **13**: 2028.
13. Röckmann T, Levin I. *J. Geophys. Res.* 2005; **110**: D21304. DOI: 10.1029/2005JD006066.
14. Yoshida N, Toyoda S. *Nature* 2000; **405**: 330.
15. Röckmann T, Kaiser J, Brenninkmeijer CAM, Crowley JN, Borchers R, Brand WA, Crutzen PJ. *J. Geophys. Res.* 2001; **106**: D10403.
16. Toyoda S, Yoshida N, Urabe T, Nakayama Y, Suzuki T, Tsuji K, Shibuya K, Aoki S, Nakazawa T, Ishidoya S, Ishijima K, Sugawara S, Machida T, Hashida G, Morimoto S, Honda H. *J. Geophys. Res.* 2004; **109**: D08308. DOI: 10.1029/2003JD004316.
17. Kaiser J, Engel A, Borchers R, Röckmann T. *Atmos. Chem. Phys. Discuss.* 2006; **6**: 4273.
18. Park S, Atlas EL, Boering KA. *J. Geophys. Res.* 2004; **109**: D01305. DOI: 10.1029/2003JD003731.
19. Yoshida N. *Nature* 1988; **335**: 528.
20. Barford CC, Montoya JP, Altabet MA, Mitchell R. *Appl. Environ. Microbiol.* 1999; **65**: 989.
21. Casciotti KL. PhD thesis, Princeton University, 2002.
22. Toyoda S, Yoshida N, Miwa T, Matsui Y, Yamagishi H, Tsunogai U, Nojiri Y, Tsurushima N. *Geophys. Res. Lett.* 2002; **29**: 7–1.
23. Sutka RL, Ostrom NE, Ostrom PH, Gandhi H, Breznak JA. *Rapid Commun. Mass Spectrom.* 2003; **17**: 738. DOI: 10.1002/rcm.968.
24. Sutka RL, Ostrom NE, Ostrom PH, Gandhi H, Breznak JA. *Rapid Commun. Mass Spectrom.* 2004; **18**: 1411. DOI: 10.1002/rcm.1482.
25. Toyoda S, Mutohe MH, Yamagishi H, Yoshida N, Tanji Y. *Soil Biol. Biochem.* 2005; **37**: 1535.
26. Sutka RL, Ostrom NE, Ostrom PH, Breznak JA, Gandhi H, Pitt AJ, Li F. *Appl. Environ. Microbiol.* 2006; **72**: 638.
27. Popp BN, Westley MB, Toyoda S, Miwa T, Dore JE, Yoshida N, Rust TM, Sansone FJ, Russ ME, Ostrom NE, Ostrom PH. *Glob. Biogeochem. Cycles.* 2002; **16**: 1064. DOI: 10.1029/2001GB001806.
28. Yamagishi H, Yoshida N, Toyoda S, Popp BN, Westley MB, Watanabe S. *Geophys. Res. Lett.* 2005; **32**: L04603. DOI: 10.1029/2004GL021458.
29. Westley MB, Yamagishi H, Popp BN, Yoshida N. *Deep Sea Res. II* 2006; DOI: 10.1016/j.dsr2.2006.03.012.
30. Pérez T, Trumbore SE, Tyler SC, Matson PA, Ortiz-Monasterio I, Rahn T, Griffith DWT. *J. Geophys. Res.* 2001; **106**: D9869. DOI: 10.1029/2000JD900809.
31. Yamulki S, Toyoda S, Yoshida N, Veldkamp E, Grant B, Bol R. *Rapid Commun. Mass Spectrom.* 2001; **15**: 1263.
32. Ueda S, Ogura N, Wada E. *Geophys. Res. Lett.* 1991; **18**: 1449.
33. Kaiser J, Röckmann T, Brenninkmeijer CAM. *J. Geophys. Res.* 2003; **108**: D4476. DOI: 10.1029/2003JD003613.
34. Kaiser J, Park S, Boering KA, Brenninkmeijer CAM, Hilker A, Röckmann T. *Anal. Bioanal. Chem.* 2004; **378**: 256. DOI: 10.1007/s00216-003-2233-2.
35. Bigeleisen J. *Science* 1965; **147**: 463.
36. Begun GM, Landau L. *J. Chem. Phys.* 1961; **35**: 547. DOI: 10.1063/1.1731966.
37. Lorquet JC, Cadet C. *Int. J. Mass Spectrom. Ion Phys.* 1971; **7**: 245. DOI: 10.1016/0020-7381(71)80020-7.
38. Märk E, Märk TD, Kim YB, Stephan K. *J. Chem. Phys.* 1981; **75**: 4446. DOI: 10.1063/1.442611.
39. Brenninkmeijer CAM, Janssen C, Kaiser J, Röckmann T, Rhee TS, Assonov SS. *Chem. Rev.* 2003; **103**: 5125. DOI: 10.1021/cr020644k.
40. Shah MS, Oza TM. *J. Chem. Soc.* 1932; 725.
41. Brower KR, Oxley JC, Tewari M. *J. Phys. Chem.* 1989; **93**: 4029.
42. Rosser WA, Inami S, Wise H. *J. Phys. Chem.* 1963; **67**: 1753.
43. Saunders HL. *J. Chem. Soc.* 1922; 698.
44. Kaiser J. PhD thesis, University of Mainz, 2002.